HHS Public Access

Author manuscript

Reprod Toxicol. Author manuscript; available in PMC 2023 April 01.

Published in final edited form as:

Reprod Toxicol. 2022 April ; 109: 121–134. doi:10.1016/j.reprotox.2022.03.007.

Inhibition of Sirtuin-1 hyperacetylates p53 and abrogates SIRT1-p53 interaction in Cr(VI)-Induced Apoptosis in the ovary

Kirthiram K. Sivakumar[1],

Jone A. Stanley[1],

Jonathan C. Behlen,

Liga Wuri,

Sudipta Dutta,

John Wu,

Joe A. Arosh,

Sakhila K. Banu[*]

Department of Veterinary Integrative Biosciences, College of Veterinary Medicine and Biomedical Sciences, Texas A&M University, College Station, TX 77843, USA

Abstract

Environmental contamination with hexavalent chromium, Cr(VI), has been increasing in the United States as well as in developing countries. Exposure to Cr(VI) predisposes the human population to various diseases, including cancer, infertility, and developmental problems in children. Previous findings from our laboratory reported that prenatal exposure to Cr(VI) caused premature ovarian failure through p53-mediated mechanisms. Sirtuin 1 (SIRT1) is an NAD+-dependent histone deacetylase class III. SIRT1 deacetylates several histones and non-histone proteins such as p53 and NFkB. The current study determines a role for the SIRT1-p53 network in apoptosis induced by Cr(VI) in the ovary and establishes physical interaction between SIRT1 and p53. Adult pregnant dams were given regular drinking water or Cr(VI) (10 ppm potassium dichromate in drinking water, *ad libitum*), and treated with SIRT1 inhibitor, EX-527 (50 mg/kg body weight, i.p.,), during 9.5 −14.5 days post-coitum. On postnatal day-1, ovaries from F1 offspring were collected for various analyses. Results indicated that Cr(VI) increased germ cell and somatic cell apoptosis, upregulated acetyl-p53, activated the apoptotic pathway, and inhibited cell survival pathways. Cr(VI) decreased acetyl-p53-SIRT1 co-localization in the ovary. In an immortalized rat granulosa cell line SIGC, Cr(VI) inhibited the physical interaction between

[*]***Address correspondence to***: **Sakhila K. Banu, PhD**., Associate Professor, Department of Veterinary Integrative Biosciences, College of Veterinary Medicine and Biomedical Sciences, Texas A&M University, College Station, Texas 77843, USA, Phone: 979-458-3613, Fax: 979-847-8981, skbanu@cvm.tamu.edu.

[1]These authors have equally contributed to this work.

Disclosure Statement: The authors have nothing to disclose.

Declaration of interests

The authors declare that they have no known competing financial interests or personal relationships that could have appeared to influence the work reported in this paper.

SIRT1 and acetyl-p53 by altering the p53:SIRT1 ratio. EX-527 exacerbated Cr(VI)-induced mechanisms. For the first time, the current study shows a novel mechanism for Cr(VI)-induced apoptosis in the ovary, mediated through the p53-SIRT1 network, suggesting that targeting the p53 pathway may be an ideal approach to rescue ovaries from Cr(VI)-induced apoptosis.

Keywords

Ovary; chromium-VI; germ cell; somatic cells; apoptosis; Sirtuin-1; EX-527; p53

1. Introduction

Hexavalent chromium, Cr(VI), has been used in various industries such as leather and textiles, metallurgical, chemical, and automobile industries [1]. Due to increased use and improper disposal of chromium, its levels in the water, soil, and air continue to rise [2, 3]. Total Cr levels in drinking water sources in developing countries such as China, India, Bangladesh, and Mexico have been recorded as high as 19–50 ppm [4–8]. Women working in dichromate manufacturing industries and tanneries and living around Cr(VI) contaminated areas have high levels of Cr in blood and urine and encounter gynecological illnesses, abortion, postnatal bleeding, and birth complications [9]. Welding fumes and metal dust containing Cr(VI) are known to be either teratogenic, carcinogenic, embryotoxic, or mutagenic [10]. Women working in electronic waste industries had high Cr levels in their blood and urine with increased abortion rates, particularly in male fetuses [11].

When we consider the U.S. population, significant contamination with Cr(VI) has been found in the drinking water sources of several cities in the U.S., exposing Americans to various adverse health effects such as cancer and infertility [12]. Environmental exposure to Cr(VI) in pregnant women in the U.S caused infertility and intra uterine fetal growth restriction (IUGR) for two generations [13]. Occupational exposure to Cr(VI) is found among approximately one-half million industrial workers in the U.S. and several million worldwide [14]. Recent literature reveals that an estimated 120,000 workers in India and 515,500 in the U.S are employed in leather tanning industries. About 300,000 workers of these industries are severely affected by chromium and its compounds worldwide per year [3].

Occupational exposure to Cr(VI) during pregnancy caused IUGR, resulting in low birth weight [10]. Previous epidemiological studies have reported an increase in the risk of spontaneous abortion among women employed in Finnish metal industries [15, 16]. The presence of Cr in umbilical cord blood and placental tissue in these women directly correlated with an increased risk of abortion [17]. High accumulation of Cr was reported in the umbilical cord blood of women exposed to Cr(VI) in electronic-waste (e-waste) processing industries in Guiyu, China (306.20 μg/L with a median level of 19.95 μg/L) [18]. Cr was detected in the amniotic fluid of diabetic women [19]. Another study reported a negative association between follicular fluid Cr and the proportion of mature MII oocytes retrieved from women who undergo IVF [20]. A study from China involving 7290 singleton live births measured maternal urinary Cr levels (low: ≤1.09 μg/g cr, middle: 1.09–3.76

μg/g cr, and high >3.76 μg/g cr [11]. Women living near Cr contaminated areas gave birth to infants with increased risk of congenital malformations, DNA damage, and low birth weight [18]. Thus, it is evident from the epidemiological data that Cr(VI) exposure severely affects the health of reproductive-age women and newborn children due to occupational and environmental exposures.

Exposure to heavy metals during pregnancy increases oxidative stress in the maternal and fetal compartments of the placenta resulting in adverse pregnancy outcomes [21, 22]. While Cr is known to affect reproductive health in women adversely, the specific mechanisms of reproductive toxicity are not clearly understood. Cr(VI) is rapidly transported through the cell membrane *via* anion transporters [23]. The reduction of Cr(VI) into Cr(V) induces DNA damage and mutations [24]. The genotoxic effects of Cr are predominantly represented by the formation of oxidative adducts and apurinic/apyrimidinic lesions, eventually resulting in DNA breaks [25]. p53 is a tumor suppressor gene that is activated by DNA damage such as radiation, oxidative stress, and chemotherapeutic drugs [26]. Under normal conditions, p53 is destabilized and degraded. However, genotoxic stress leads to the stabilization of p53 through various mechanisms. As a result, p53 accumulates inside cells, inducing cell cycle arrest, senescence, and apoptosis [27].

Sirtuin 1 (SIRT1), an NAD^+-dependent histone deacetylase class III, is one of the seven mammalian sirtuins. SIRT1 plays multiple and diverse roles in metabolism, development, stress response, neurogenesis, hormone responses, and apoptosis [28, 29]. SIRT1 is recognized as an anti-aging protein [30, 31]. Interestingly, a SIRT1 activator (SRT1720) was reported to improve the follicle reserve and prolong the ovarian lifespan of diet-induced obesity in female mice [32]. Resveratrol, an activator of SIRT1, has an anti-aging effect and is beneficial to the cardiovascular system, diabetes, and obesity [33]. Consistently, it prolonged the ovarian lifespan and protected against age-associated infertility in rodents [34, 35]. Our previous report showed that resveratrol protected the ovary against Cr(VI)-toxicity in pre-pubertal rats by enhancing endogenous antioxidant enzymes and inhibiting the metabolic clearance of estradiol [36].

SIRT1 deacetylates non-histone proteins such as p53, FOXO), and NFkB [29, 37–40]. SIRT1 activates the PPARγ coactivator 1-alpha (PGC-1α) and increases the expression of antioxidants such as superoxide dismutase (SOD) and glutathione peroxidase (GSH-Px) [41, 42]. PGC-1α is a transcriptional coactivator, which regulates mitochondrial biogenesis [43]. Various endocrine disrupting chemicals (EDCs) such as lead [44] and fluoride [45] negatively regulates SIRT1, promoting oxidative damage to the central nervous system. SIRT1 acetylation regulates key signaling pathways perturbing mitochondrial function [46]. In Alzheimer's disease, the β-amyloid protein content in the brain is negatively correlated with the SIRT1 content [47, 48]. SIRTI can activate Nrf2 transcriptional activity and upregulate the expression of SOD and GSH downstream of Nrf2 [49]. Deacetylation of p53 by SIRT1 decreases apoptosis mediated by oxidative stress [39]. SIRT1 colocalizes with p53 in promyelocytic leukemia nuclear bodies [50, 51] where it deacetylates p53 and antagonizes p53-mediated cellular senescence [51]. Though SIRT1 plays a vital role in negatively regulating p53, its role in the ovary of the offspring in response to *in utero* exposure has not been understood. Therefore, we *hypothesize that Cr(VI)-induced apoptosis*

in the ovary is regulated through the p53-SIRT1 network. The objective of the current study is to test this hypothesis in the ovaries of F1 pups exposed to Cr(VI) *in utero*.

2. Materials and methods

2.1. Chemicals

All our chemicals and cell culture reagents were purchased from Millipore-Sigma (St. Louis, MO) or Thermo Fisher Scientific (Waltham, MA). Antibodies (Table.1) were obtained from Abcam (Cambridge, MA). Spontaneously Immortalized Granulosa Cells (SIGC) were received from Dr. Burghardt, Professor & Director, Image Analysis Laboratory, College of Veterinary Medicine & Biomedical Sciences, Texas A&M University.

2.2. In vivo dosing of the animals

Pregnant Sprague-Dawley rats of 60–70 days of age were divided into four groups. Briefly, control rats received regular drinking water and diet *ad libitum*. Whereas the rats from the treatment groups received SIRT1 inhibitor EX-527 (50 mg/kg body weight), with or without 10 ppm Cr(VI) (potassium dichromate). Cr(VI) treatment was given through the drinking water, while EX-527 was given by intraperitoneal injections every day. All the rats received Cr(VI) with or without EX-527 injections from gestational day (GD) 9.5 to 14.5. The rats were allowed to deliver pups (F1 offspring), and the ovaries were removed on PND 1 for further analyses. Animal use protocols were performed following the National Institutes of Health Guidelines for the Care and Use of Laboratory Animals, were in accordance with the standards established by Guiding Principles in the Use of Animals in Toxicology and specific guidelines and standards of the Society for the Study of Reproduction and were approved by the Institutional Animal Care and Use Committee of Texas A&M University.

2.3. Rationale for choosing Cr doses for the in vivo study

The EPA has established a maximum contaminant level (MCL) of 100 μg/L or 100 ppb for total chromium in drinking water. Groundwater from Midland, Texas, contains 5.28 ppm Cr (5280 μg/L) [31]. A study conducted in Piedmont aquifers of North Carolina documented that 90% of the wells had detectable Cr(VI) and were above the California public health goal, 0.02 μg/L [52]. The chromium in groundwater in India ranges from 0.01–16.30 ppm [53]. Shockingly, blood Cr levels in workers of developing countries were reported follows: Bangladesh: 26.97 μg/L; Pakistan: 16 μg/L; India: 147 μgL; Kenya: 63 μg/L; Chinese: 2500 μg/L [3]. In general, humans are exposed to as much as 10 ppm Cr(VI) in drinking water from contaminated wells [54]. Therefore, we chose 10 ppm Cr(VI) for the current study.

2.4. In vitro treatment of SIGC cells

Culture of Spontaneously Immortalized rat Granulosa Cell line: A spontaneously immortalized rat granulosa cell line (SIGC) [55] was cultured in DMEM-F12 (Sigma, Saint Louis, MO) supplemented with 5% Dextran Charcoal coated-Fetal Bovine Serum (DC-FBS) (Hyclone, Logan, UT), penicillin 100 U/ml, streptomycin (100 μg/ml) and amphotericin-B (2.5 μg/ml) in a humidified atmosphere with 95% air, 5% CO_2 at 37°C. At 70% confluency, SIGC were serum-starved for 24 h and incubated in DMEM-F12 supplemented with 2% DC-FBS (in base medium) in the presence or absence of Cr(VI) (25

μM potassium dichromate) for 12 h or 24 h. After the treatment, cells were harvested using 0.1% trypsin-EDTA, and total protein was isolated for immunoprecipitation (IP) and western blot analyses.

2.5. Immunohistochemistry and image quantification by Image-ProPlus software

Paraffin sections from the ovary were fixed in 4% buffered paraformaldehyde containing 6 g PFA, 325 mg NaOH, 15 ml 103 PBS in 100 ml diethyl pyrocarbonate-treated double-distilled H2O, pH 7.2, for 4 h at 48C and processed using Vectastain Elite ABC kit (Vector Laboratories). An avidin/biotin-based peroxidase system was used to detect the biotinylated secondary antibody, and the sections were developed using the chromogen 3-amino-9-ethylcarbazole, a peroxidase substrate that produces an insoluble end product that is red in color and observed visually. Sources of antibodies, catalog numbers, dilution, host species, immunogen, and homology with rat/mouse/human are given in Table-1. Digital images were captured at 400x magnification using a Zeiss Axioplan 2 Research Microscope (Carl Zeiss, Thornwood, NY) with an Axiocam HR digital color camera. The intensity of staining for each protein was quantified using Image-ProPlus 10.0.8 software according to the manufacturer's instructions (Media Cybernetics, Inc.; Bethesda, MD), described in the literature [56], and our previous findings [21, 36, 57]. The average staining intensity of multiple ovaries was calculated from the litters of treated dams (n=5). Integrated Optical Density (IOD) of immunostaining was quantified in the RGB mode. Numerical data were expressed as mean ± SEM.

2.6. TUNEL assay and histology

Paraffin-embedded tissue sections were deparaffinized, and TUNEL assay was performed as we described [57, 58]. The apoptosis index (AI) was calculated as the average percentage of TUNEL-positive cells from the ovaries (n=8) at magnification x400 [36]. Histology and H&E staining of the tissue sections were performed at the College of Veterinary Medicine and Biomedical Sciences core histology laboratory, Texas A&M University.

2.7. Isolation of protein

After the treatments, the total protein from the cells was isolated for immunoblotting. Briefly, the cells were harvested using 1% Trypsin-EDTA and pelleted by centrifuging at 13, 200 rpm for 10 minutes at 4°C. The cell lysates were sonicated in sonication buffer (20 mM Tris–HCl, 0.5 mM EDTA, 100 μM DEDTC, 1% Tween, 1mM phenylmethylsulfonyl fluoride, and protease inhibitor cocktail tablets (EDTA-free) (1 tablet/50 ml) and PhosSTOP Phosphatase Inhibitor Cocktail Tablets (1 tablet/10 ml) (Millipore Sigma, Burlington, MA). Sonication was performed using a Microson ultrasonic cell disruptor (Microsonix Incorporated, Farmingdale, NY). After sonication, the samples were centrifuged at 13,200 rpm for 15 minutes at 4°C. The supernatant was recovered, and protein concentration was determined using the Bradford method and a Bio-Rad Protein Assay kit (BIO-RAD, Hercules, CA).

2.8. Immunofluorescence

Paraffin-embedded sections of the PND1 ovaries were deparaffinized in xylene and dehydrated in a graded ethanol series: 100%, 95%, and 70% for 5 min followed by washing in 1xPBS. Antigen retrieval was performed by incubating the sections in a protease solution (100 mg of protease in 200 ml of 1x PBS) for 5 min at 37°C and washed three times in double-distilled water and once in PBS. Subsequently, the tissues were permeabilized by washing the sections twice for 10 minutes with 1% goat serum in PBST (PBS containing 0.4% Triton X-100) and incubated with blocking buffer (PBS containing 0.4% Triton X-100 and 5% goat serum) for one h at room temperature. The sections were incubated overnight at 4 °C with rabbit polyclonal antibodies specific for p53 and SIRT1. The following day, the sections were washed in PBST three times and incubated with Alexa Fluor 488-conjugated goat anti-rabbit secondary antibody and Alexa Fluor 594-conjugated goat anti-mouse secondary antibody at 1:200 dilutions for one h at room temperature. The proper negative control is used by substituting serum at the same concentration as the primary antibody [59]. The sections were washed with PBST and mounted using ProLong Gold antifade reagent (Invitrogen, Eugene, Oregon). The slides were kept in the dark overnight at room temperature. Confocal images were captured using a Zeiss 510 Meta multiphoton/ confocal microscope (Carl Zeiss) with a plan apochromat 633/1.4 NA oil objective. An argon laser set was used for the fluorophore with an excitation of 488 nm and emission (collected with a band-pass filter) of 500–550 nm. A helium-neon laser was used for the red dye with an excitation of 543 nm and emission (collected with a long-pass filter) of 560 nm. At least eight images were collected per treatment.

2.9. Immunoprecipitation

Immunoprecipitation (IP) was carried out using protocols provided by Cell Signaling Technology and as published [60]. Briefly, total cell lysate (1 mg, ~120–125 μl) was precleared by incubating with ImmunoCruz F pre-clearing matrix B-rabbit (50μl/ml) (Cat. SC-45057, Santa Cruz Biotechnology, Santa Cruz, CA) for 30 min at 4°C. After incubation, the matrix was pelleted by microcentrifugation at 1000 rpm for 1 min at 4° C. The pellet was discarded, and the precleared lysate (~120–125 μl) was incubated with rabbit oligoclonal acetyl-p53 (K-382) antibody (1μg/ml) (Cat. 710294, Thermo Fisher Scientific) overnight at 4°C with rotation. After overnight incubation, the mixture was further incubated with ImmunoCruz F IP matrix (50 μl/ml) (Cat. SC-45043, Santa Cruz Biotechnology, Santa Cruz, CA) overnight at 4°C. Protein-antibody IP complexes were precipitated and washed with 500μl of IP buffer: 20mM Tris-HCl, 0.5mM EDTA, 100 μM DEDTC, 1% Tween, 1 mM phenyl methyl sulfonyl fluoride, and protease inhibitor cocktail tablets, that is, complete EDTA-free (1 tablet/50 ml) and PhosStop (1 tablet/10 ml). Finally, the protein-antibody IP complexes were resuspended in 40μl of 2× SDS sample buffer, boiled at 100°C for 5–10 min, and resolved in 10% SDS PAGE gel. Rabbit IgG was immunoprecipitated and was used as an internal control.

2.10. Western blotting

Approximately 75 μg aliquots of total proteins were loaded in each lane and electrophoresed on 10% SDS polyacrylamide gels, then electrotransfer onto nitrocellulose membranes

(Amersham Pharmacia Biotech, Chicago, IL). Prestained protein markers (Fisher, BP3603–1) were used as molecular weight standards for each analysis. The blots were stained with 0.5% ponceau-stain in 1% acetic acid for evaluating the quality of protein transfer. Proteins were blocked overnight at 4°C with 5% fat-free dry milk powder in PBS and 0.05% Tween-20 (PBST). The blots were incubated with SIRT1 primary antibody for 12 h at 4°C at a dilution of 1:1000 in 2% fat-free dry milk powder in PBST. The blots were washed three times at 10-min intervals in PBS-T and then incubated with secondary antibody (goat anti-rabbit IgG conjugated with horseradish peroxidase (Jackson Immunoresearch Laboratories, West Grove, PA) for one h at room temperature at a dilution of 1:10,000 in 2% fat-free dry milk powder in PBS-T. Blots were then washed three times at 10-min intervals in PBS-T. A chemiluminescent substrate (SuperSignal West Femto Maximum Sensitivity Substrate) was applied according to the manufacturer's instructions (Cat. No. 34094, Pierce Biotechnology, Rockford, lL). The blots were exposed to Blue X-Ray film, and densitometry of autoradiograms was performed using an Alpha Imager (Alpha Innotech Corporation, San Leandro, CA). Sources of antibodies, catalog numbers, dilution, host species, immunogen, and homology with rat/mouse are given in Table 1.

2.11. Statistical analysis

All the numerical data were subjected to one-way ANOVA to detect the effects of treatments and interactions. The Tukey-Kramer HSD test was used to adjust for multiple pair-wise comparisons of means. We consider the nested structure in the design. Mixed models analysis was used to account for any correlation between the results of pups from the same dam. Mixed models were used to model both fixed effects (in this case, treatment) and random effects (in this case, dams and pups) [61]. Statistical analyses were performed using general linear models of the Statistical Analysis System (SAS, Cary, NC), and $p \leq 0.05$ was considered significant.

3. Results

3.1. Inhibition of SIRT1 increased germ cell apoptosis

Prenatal exposure to Cr(VI) significantly ($p<0.05$) increased germ cell apoptosis compared to the control group (Fig. 1A, B & G). Treatment with EX-527 alone increased apoptosis in the ovary compared to the control (Fig. 1A, C & G). Combined treatment with EX-527 and Cr(VI) showed a significant ($p<0.05$) additive effect on apoptosis compared to Cr(VI) or EX-527 treatment alone (Fig. 1B–D&G). Figures 1E and 1F represent H&E sections of the control and Cr(VI)-exposed ovaries, respectively. Control ovaries have healthy oocytes intact and arranged inside the germ cell nests (GCN). Interestingly, Cr(VI) advanced GCN breakdown by increasing germ cell apoptosis. Advanced GCN breakdown led to disintegrated GCN and (partially) formed primordial follicles (Fig. 1F, white arrows). Control ovaries did not show any primordial follicles. Arrows (black) indicate germ cells, and the arrowheads indicate a somatic cell and white arrows indicate partially formed primordial follicles.

3.2. Inhibition of SIRT1 increased p53 acetylation

Our previous finding indicated that Cr(VI) exposure increased total p53 in the PND1 ovary [58]. The EX-527 (Sirt1 inhibitor) treatment increased acetylation of p53 (at Lysine - 382) after DNA damage in primary human mammary epithelial cells [62]. To understand if Cr(VI) hyper acetylates p53, we studied the expression acetyl-p53 in the ovaries exposed to Cr(VI). Data indicated that exposure to Cr(VI) significantly ($p<0.05$) increased the levels of acetyl-p53(K-382) compared to control (Fig. 2A, B & E). EX-527 significantly ($p<0.05$) increased acetyl-p53 (K-382) expression in PND1 ovaries compared to control (Fig. 2A, C & E). It is also evident that while acetyl-p53 was predominantly expressed in the oocytes of the Cr(VI) treated ovaries, it is mainly expressed in the somatic cells of the EX-527 treated ovaries. Thus, a spatio-temporal expression pattern of the acetyl-p53 was observed. Combined treatment with Cr(VI) and EX-527 showed a significant ($p<0.05$) additive effect and increased acetyl-p53 in PND1 ovaries compared to Cr(VI) or EX-527 treatment alone (Fig. 2B–E). Arrows indicate germ cells, and the arrowhead indicates a somatic cell.

3.3. Inhibition of SIRT1 increased cleaved caspase-3

Our findings indicated that Cr(VI) caused apoptosis of germ cells [58, 63] and trophoblasts [64] through caspase-3 dependent mechanisms. Treatment with Cr(VI) or EX-527 significantly ($p<0.05$) increased the expression of cleaved caspase-3 (Fig. 3A, B, C & E) in PND1 ovaries compared to control. Combined treatment with Cr(VI) and EX-527 showed a significant ($p<0.05$) synergistic effect compared to Cr(VI) or EX-527 treatment alone (Fig. 3B–E). Arrow indicates germ cell, and the arrowhead indicates a somatic cell.

3.4. Inhibition of SIRT1 increased Bax

Bax regulates the primordial germ cell survival and apoptosis in mice [77]. Bax mutant mice exhibited three times larger follicle pool compared to wild-type mice [78]. To understand the regulation of Bax through SIRT1, we studied Bax expression in the ovaries exposed to Cr(VI) and/or EX-527. Exposure to Cr(VI) significantly ($p<0.05$) increased the expression of BAX compared to control (Fig. 4A, B & E), whereas EX-527 and Cr(VI) showed a significant ($p<0.05$) synergistic effect on Bax expression compared to Cr(VI) or EX-527 treatment alone (Fig. 4B–E). Arrow indicates germ cell, and the arrowhead indicates a somatic cell.

3.5. Inhibition of SIRT1 increased p53-upregulated modulator of apoptosis (PUMA)

The p53 upregulated modulator of apoptosis (PUMA) is a pro-apoptotic protein (encoded by the Bbc3 gene), a member of the BCL-2 protein family. The expression of PUMA is regulated by p53. We have previously identified PUMA as a crucial effector for p53 in Cr(VI)-induced trophoblast apoptosis [22]. Other studies also have shown that elimination of PUMA partly rescued ovarian reserve from γ-irradiation [65] and fully rescued the entire primordial follicle pool against DNA-damaging chemotherapeutic agents [66]. To understand if PUMA is the downstream effector of p53 in mediating apoptosis, we studied PUMA. Treatment with either Cr(VI) (Fig. 5A, B & E) or EX-527 (Fig. 5C & E) significantly ($p<0.05$) increased the expression of PUMA in PND1 ovaries compared to control. However, combined treatment with Cr(VI) and EX-527 had a significant ($p<0.05$)

synergistic effect on Cr(VI)-induced apoptosis compared to Cr(VI) or EX-527 treatment alone (Fig. 5B–E). Arrow indicates germ cell, and the arrowhead indicates a somatic cell.

3.6. Inhibition of SIRT1 downregulated Bcl-2

B-cell lymphoma 2 (Bcl2) is a vital cell survival protein that prevents apoptosis by directly binding and inhibiting the pro-apoptotic Bax and Bak [67]. Overexpression of Bcl2 in the oocytes increased the size of the primordial follicle pool at birth in mice [68]. To understand if Bcl2 is regulated through SIRT1, Bcl2 expression was studied in the ovaries exposed to the SIRT1 inhibitor. Bcl2 was abundantly expressed in the control ovaries (Fig. 6A), whereas Cr(VI) significantly ($p<0.05$) decreased Bcl2 expression compared to control (Fig. 6A, B & E). Treatment with EX-527 alone decreased the expression of Bcl2 (Fig. 6C & E). Treatment with EX-527 and Cr(VI) showed a significant ($p<0.05$) additive effect compared to Cr(VI) or EX-527 treatment alone (Fig. 6B–E). Arrow indicates germ cell, and the arrowhead indicates a somatic cell.

3.7. Inhibition of SIRT1 downregulated Bcl-XL

B-cell lymphoma-extra-large (Bcl-XL) is an anti-apoptotic protein that plays a crucial role in determining germ cell fate in early gonadal development, and it has an active role in protecting human ovarian cells from apoptosis [69]. Mice deficient in Bcl-XL showed a decrease in primordial follicles compared to wild-type mice [70]. To understand if Bcl-XL is regulated through SIRT1, Bcl-XL expression was studied in the ovaries exposed to EX-527. Bcl-XL was abundantly expressed in the control ovaries (Fig. 7A). Cr(VI) (Fig. 7A, B & E) or EX-527 (Fig. 7C & E) significantly ($p<0.05$) decreased the expression of Bcl-XL compared to control. EX-527 accelerated Cr(VI)-induced decrease in Bcl-XL ($p<0.05$) (Fig. 7B–E). Arrow indicates germ cell, and the arrowhead indicates a somatic cell.

3.8. Inhibition of SIRT1 downregulated phospho-AKT

Phosphatidylinositol-4,5-bisphosphate 3-kinase (PI3K)/AKT pathway is significant for the survival, dormancy and activation of the primordial follicle and any disruption of the AKT pathway could lead to infertility [71]. AKT is the critical regulator of cell survival and proliferation [72]. To understand if AKT is regulated through SIRT1, p-AKT expression was studied in the ovaries exposed to EX-527. Cr(VI) significantly ($p<0.05$) decreased pAKT expression (Fig. 8A, B & E) compared to control. Treatment with EX-527 alone significantly ($p<0.05$) reduced pAKT expression (Fig. 8C & E). However, treatment with Cr(VI) and EX-527 did not show an additive or synergistic effect compared to Cr(VI) or EX-527 treatment alone (Fig. 8B–E). Arrow indicates germ cell, and the arrowhead indicates a somatic cell.

3.9. Inhibition of SIRT1 altered acetyl p53-SIRT1 interaction and increased p53: SIRT1 ratio

Previous findings from our laboratory demonstrated that Cr(VI) increased total p53 expression in the ovary and placenta [22, 58]. Current data indicate that Cr(VI) increased acetyl-p53 expression on the same cells that undergo apoptosis. However, Cr(VI) effects on p53-SIRT1 interaction could be due to decreased SIRT1 or increased p53 or decreased

p53: SIRT1 ratio. To understand the exact mechanism of SIRT1-mediated regulation of p53, we conducted three experiments. *Experiment 1*: Acetyl-p53 and SIRT-1 were co-localized in control and Cr(VI)-treated ovaries. Cr(VI) increased acetyl p53:SIRT1 ratio (Fig. 9H), and decreased p53-SIRT-1 co-localization (Fig. 9G). *Experiment 2*: IHC was performed with control and Cr(VI)-treated ovaries to detect SIRT1 protein expression. Cr(VI) significantly decreased ($p<0.05$) SIRT1 expression in the ovary (Fig. 10A–C). *Experiment 3:* To have a mechanistic insight of SIRT1-p53 interaction, SIGC cells were used as a model system. Immunoprecipitation (IP) studies showed that Cr(VI) significantly decreased ($p<0.05$) the interaction between acetyl p53-SIRT1 (Fig. 10D & E), thus rescuing p53 from SIRT1-induced deacetylation and inactivation. However, future studies would further confirm such an association in the germ cells or oocytes using IP studies.

4. Discussion

The previous report from our laboratory indicated that prenatal exposure to Cr(VI) induced premature ovarian failure in the F1 offspring by increasing germ cell apoptosis [70]. Several of our studies have identified p53 as one of the critical regulators for Cr(VI)-induced apoptosis of ovarian germ cells and trophoblasts. The current study indicated that prenatal exposure to Cr(VI) caused apoptosis of germ cells and somatic cells during fetal ovarian development in F1 offspring through the activation of the p53 pathway by hyperacetylating (and stabilizing) the p53. Cellular stress can cause several changes in p53 protein by post-translational modifications such as ubiquitination, phosphorylation, and acetylation. Acetylation of p53 on the C-terminal domain abrogates its ubiquitination by Mdm2, stabilizing the p53 protein [73]. However, whether such a mechanism exists in *in-utero* exposure to EDCs is not clear. Interestingly, the current study is novel as it indicates that gestational exposure to Cr(VI) stabilized p53 in the neonatal ovaries by increasing its acetylation, resulting in germ cell apoptosis. Moreover, we observed a differential staining pattern for acetyl-p53 between Cr(VI) and EX-527 ovaries. While acetyl p53 is predominantly detected in the oocytes of the Cr(VI) exposed rats, it is expressed more in somatic cells of the EX-527 treated rats. Cr(VI) accelerated germ cell nest (GCN) breakdown, and an advanced GCN breakdown leads to the increased intrusion of somatic cells around the individual oocytes, beginning follicle assembly. This could be the possible reason for the differential staining pattern between the groups Cr(VI) and EX-527.

SIRT1 is a highly conserved NAD^+-dependent protein deacetylase that participates in several cellular functions, including apoptosis and oxidative and genotoxic stress. SIRT1 protects and promotes cell survival against oxidative stress and DNA damage. Upon activation, SIRT1 deacetylates histones and histone methyltransferases and a variety of non-histone target proteins, including p53. As shown by the current study (Fig. 10) and in the model diagram (Fig. 11), SIRT1 physically interacts with p53 and deacetylates p53 at Lys-382. In the presence of SIRT1, cells can escape p53-mediated apoptosis. On the other hand, in the absence or decrease of SIRT1, p53 remained acetylated and stabilized as an active form. Our data indicated that Cr(VI) had (i) decreased the expression of SIRT1; therefore, SIRT1's ability to deacetylate p53 was minimized; (ii) increased the expression of p53, thus increasing its availability; (iii) hyperacetylated p53; (iv) altered the ratio of p53:SIRT1, and (v) decreased physical interaction between p53 and SIRT1. For the first

time, our data reveal an association between SIRT1 and p53 in Cr(VI)-induced germ cell apoptosis.

PUMA is an essential downstream candidate for p53-mediated apoptosis. PUMA is a critical regulator of germ cell death during ovarian development. PUMA-mediated cell death limits the primordial follicle number established in the initial ovarian reserve [65–66]. In particular, Cr(VI) caused apoptosis of germ cells, granulosa cells, and trophoblasts by upregulating PUMA [30, 71]. During UV-induced apoptosis, PUMA promotes the translocation of BAX by interacting with BAX directly [77]. Our results show that SIRT1inhibitor significantly increased PUMA. Our data indicate that exposure to Cr(VI) induced apoptosis by activating the p53-PUMA-BAX-caspase-3 cascade in the F1 ovary.

Bcl-2 promotes cell survival by inhibiting caspases. Overexpression of Bcl-2 protein in the ovary leads to decreased ovarian somatic cell apoptosis and enhanced folliculogenesis in transgenic animals [68]. Strikingly, a study from human fetal ovarian tissue spanning the period between 12 and 38 gestational weeks indicated that the highest incidence of apoptotic germ cells coincides with the lack of detectable Bcl-2 protein [74]. In the current study, cell survival proteins Bcl-2 and Bcl-XL are abundantly expressed in control ovaries; and Cr(VI) downregulated both Bcl-2 and Bcl-XL. Interestingly, SIRT1 inhibitor EX-527 down-regulated Bcl-2 and Bcl-XL, accelerating apoptosis of the germ cells and somatic cells, suggesting SIRT1 effects on cell survival machinery. Phosphorylation of AKT protects the cells from apoptosis. Granulosa cell-derived stem cell factor/kit ligand binds to the Kit receptor at the oocyte's surface and activates the PI3 kinase pathway of the oocytes. Activating PI3 kinase in the oocytes leads to the phosphorylation of the serine/threonine kinase AKT in mouse and rat oocytes, resulting in AKT activation [75]. PI3k/AKT pathway is crucial for follicular activation and development. Our study shows that Cr(VI) decreased p-AKT expression in the F1 ovary, compromising germ cell survival.

Finally, we determined the physical interaction between SIRT1 and p53. Cr(VI) decreased the colocalization of p53 and SIRT1 in the ovary by decreasing the p53:SIRT1 ratio. Data from co-immunoprecipitation using the rat granulosa cells SIGC indicated that SIRT1 physically interacts with p53. Interestingly, Cr(VI) decreased the physical interaction between SIRT1 and p53 by altering their ratio resulting in an increased abundance and stabilization of p53. It is noteworthy that Cr(VI) induced significant cell death in the ovaries, which may have partly decreased SIRT1 expression. Thus, data suggest that Cr(VI)-induced apoptosis in the ovary may partly be due to decreased SIRT1 besides its failure to interact with p53. Another study indicated that tenovin-6, a small molecule inhibitor of SIRT1, promoted p53 hyperacetylation and activation in cancer cells [76]. Thus, Cr(VI) exposure in utero stabilizes p53 in the F1 ovary promoting apoptosis. Therefore, the study suggests that in utero exposure to Cr(VI) can cause potential damage to the ovarian reserve in the early life stages of the offspring.

In conclusion, as depicted in the schematic diagram (Fig. 11), the current study indicates that prenatal exposure to Cr(VI): (i) altered p53:SIRT1 ratio and p53-SIRT1 interaction; (ii) increased the abundance of acetyl-p53; (iii) increased levels of acetyl-p53 escapes ubiquitination, becomes stable and activates its downstream candidates PUMA, Bax, and

cleaved-caspase-3; (vi) downregulates cell survival machinery Bcl-2, Bcl-XL, and p-Akt. SIRT1 inhibitor EX-527 either additively or synergistically exacerbates Cr(VI) effects. Our study suggests that targeting p53 may be ideal for rescuing ovaries from Cr(VI)-induced apoptosis.

Acknowledgments

This work was partly supported by the National Institute of Environmental Health Sciences (NIEHS) grants 1R01ES025234-01 (S.K.B) and by the Texas A&M Center for Environmental Health Research (TiCER) P30-ES029067. The authors acknowledge Dr. Robert C Burghardt, Professor and Director of the Image Analysis Laboratory (IAL), for providing the cell line SIGC. We also acknowledge Dr. Rola Barhoumi, Research Professor and Associate Director of the IAL, College of Veterinary Medicine and Biomedical Sciences, College Station, Texas, for assistance with imaging.

References

[1]. Banu S, Heavy metals and the ovary, in: Hoyer PB (Ed.), Ovarian Toxicology, CRC Press, Taylor & Francis Inc., 2013.

[2]. OSHA, Occupational exposure to hexavalent chromium. Final rule, Federal register 71(39) (2006) 10099–385. [PubMed: 16528853]

[3]. Dubey R, Verma P, Kumar S, Cr (III) genotoxicity and oxidative stress: an occupational health risk for leather tannery workers of South Asian developing countries, Toxicol. Ind. Health (2022), 07482337211055131.

[4]. Sharma P, Bihari V, Agarwal SK, Verma V, Kesavachandran CN, Pangtey BS, Mathur N, Singh KP, Srivastava M, Goel SK, Groundwater contaminated with hexavalent chromium [Cr (VI)]: a health survey and clinical examination of community inhabitants (Kanpur, India), PLoS One 7 (10) (2012), e47877. [PubMed: 23112863]

[5]. Armienta-Hernandez A, Rodriguez-Castillo R, Environmental exposure to chromium compounds in the valley of Leon, Mexico, Environ. Health Perspect 103 (1995) 47–51.

[6]. Rao GT, Rao VG, Ranganathan K, Surinaidu L, Mahesh J, Ramesh G, Assessment of groundwater contamination from a hazardous dump site in Ranipet, Tamil Nadu, India, Hydrogeol. J 19 (8) (2011) 1587–1598.

[7]. Ahmad JU, Goni MA, Heavy metal contamination in water, soil, and vegetables of the industrial areas in Dhaka, Bangladesh, Environ. Monit. Assess 166 (1–4) (2010) 347–357. [PubMed: 19521788]

[8]. Beaumont JJ, Sedman RM, Reynolds SD, Sherman CD, Li LH, Howd RA, Sandy MS, Zeise L, Alexeeff GV, Cancer mortality in a Chinese population exposed to hexavalent chromium in drinking water, Epidemiology 19 (1) (2008) 12–23. [PubMed: 18091413]

[9]. Shmitova L, Content of hexavalent chromium in the biological substrates of pregnant woen and women in the immediate postnatal period engaged in the manufacture of chromium compounds, Gig Trud Prof Zabol 2 (1980) 32–35.

[10]. Quansah R, Jaakkola JJ, Paternal and maternal exposure to welding fumes and metal dusts or fumes and adverse pregnancy outcomes, Int. Arch. Occup. Environ. Health 82 (4) (2009) 529–537. [PubMed: 18820944]

[11]. Pan X, Hu J, Xia W, Zhang B, Liu W, Zhang C, Yang J, Hu C, Zhou A, Chen Z, Cao J, Zhang Y, Wang Y, Huang Z, Lv B, Song R, Zhang J, Xu S, Li Y, Prenatal chromium exposure and risk of preterm birth: a cohort study in Hubei, China, Sci. Rep 7 (1) (2017) 3048. [PubMed: 28596517]

[12]. Andrews D, Erin Brockovich Carcinogen in Tap Water of More Than 200 Million Americans, Environmental Working Group, 2016, pp. 1–13.

[13]. Remy LL, Byers V, Clay T, Reproductive outcomes after non-occupational exposure to hexavalent chromium, Willits California, 1983–2014, Environ. Health 16 (1) (2017) 18. [PubMed: 28264679]

[14]. Salnikow K, Zhitkovich A, Genetic and epigenetic mechanisms in metal carcinogenesis and cocarcinogenesis: nickel, arsenic, and chromium, Chem. Res. Toxicol 21 (1) (2008) 28–44. [PubMed: 17970581]

[15]. Hemminki K, Niemi ML, Koskinen K, Vainio H, Spontaneous abortions among women employed in the metal industry in Finland, Int. Arch. Occup. Environ. Health 47 (1) (1980) 53–60. [PubMed: 7429646]

[16]. Hemminki K, Niemi ML, Kyyronen P, Kilpikari I, Vainio H, Spontaneous abortions and reproductive selection mechanisms in the rubber and leather industry in Finland, Br. J. Ind. Med 40 (1) (1983) 81–86. [PubMed: 6824605]

[17]. Grant K, Goldizen FC, Sly PD, Brune MN, Neira M, van den Berg M, Norman RE, Health consequences of exposure to e-waste: a systematic review, Lancet Glob. Health 1 (6) (2013) e350–e361. [PubMed: 25104600]

[18]. Li Y, Xu X, Liu J, Wu K, Gu C, Shao G, Chen S, Chen G, Huo X, The hazard of chromium exposure to neonates in Guiyu of China, Sci. Total Environ 403 (1–3) (2008) 99–104. [PubMed: 18603282]

[19]. Conner E, Cassady G, 841 amniotic fluid chromium (AFCr) in infants of diabetic mothers, Pediatr. Res 12 (4) (1978), 504–504.

[20]. Ingle ME, Bloom MS, Parsons PJ, Steuerwald AJ, Kruger P, Fujimoto VY, Associations between IVF outcomes and essential trace elements measured in follicular fluid and urine: a pilot study, J. Assist. Reprod. Genet 34 (2) (2017) 253–261. [PubMed: 27943108]

[21]. Banu SK, Stanley JA, Sivakumar KK, Taylor RJ, Arosh JA, Burghardt RC, Highlight: Exposure to CrVI during early pregnancy increases oxidative stress and disrupts the expression of antioxidant proteins in placental compartments, Toxicol. Sci 155 (2) (2017) 497–511. [PubMed: 28077780]

[22]. Banu SK, Stanley JA, Taylor RJ, Sivakumar KK, Arosh JA, Zeng L, Pennathur S, Padmanabhan V, Sexually dimorphic impact of chromium accumulation on human placental oxidative stress and apoptosis, Toxicol. Sci 161 (2) (2018) 375–387 [PubMed: 29069462]

[23]. Saha R, Nandi R, Saha B, Sources and toxicity of hexavalent chromium, J. Coord. Chem 64 (10) (2011) 1782–1806.

[24]. Zhitkovich A, Importance of chromium-DNA adducts in mutagenicity and toxicity of chromium (VI), Chem. Res. Toxicol 18 (1) (2005) 3–11. [PubMed: 15651842]

[25]. Casadevall M, da Cruz Fresco P, Kortenkamp A, Chromium(VI)-mediated DNA damage: oxidative pathways resulting in the formation of DNA breaks and abasic sites, Chem. Biol. Interact 123 (2) (1999) 117–132. [PubMed: 10597905]

[26]. Sakaguchi K, Herrera JE, Saito Si, Miki T, Bustin M, Vassilev A, Anderson CW, Appella E, DNA damage activates p53 through a phosphorylation–acetylation cascade, Genes Dev. 12 (18) (1998) 2831–2841. [PubMed: 9744860]

[27]. Fridman JS, Lowe SW, Control of apoptosis by p53, Oncogene 22 (2003) 9030–9040. [PubMed: 14663481]

[28]. Michan S, Sinclair D, Sirtuins in mammals: insights into their biological function, Biochem. J 404 (1) (2007) 1–13. [PubMed: 17447894]

[29]. Kim DH, Jung YJ, Lee JE, Lee AS, Kang KP, Lee S, Park SK, Han MK, Lee SY, Ramkumar KM, SIRT1 activation by resveratrol ameliorates cisplatin-induced renal injury through deacetylation of p53, Am. J. Physiol 301 (2) (2011) F427–F435.

[30]. Ghosh HS, The anti-aging, metabolism potential of SIRT1, Curr. Opin. Investig. Drugs 9 (10) (2008) 1095–1102.

[31]. Westphal CH, Dipp MA, Guarente L, A therapeutic role for sirtuins in diseases of aging? Trends Biochem. Sci 32 (12) (2007) 555–560. [PubMed: 17980602]

[32]. Zhou X-L, Xu J-J, Ni Y-H, Chen X-C, Zhang H-X, Zhang X-M, Liu W-J, Luo L-L, Fu Y-C, SIRT1 activator (SRT1720) improves the follicle reserve and prolongs the ovarian lifespan of diet-induced obesity in female mice via activating SIRT1 and suppressing mTOR signaling, J. Ovarian Res 7 (1) (2014) 97. [PubMed: 25330910]

[33]. Szkudelska K, Szkudelski T, Resveratrol, obesity and diabetes, Eur. J. Pharmacol 635 (1–3) (2010) 1–8. [PubMed: 20303945]

[34]. Liu M, Yin Y, Ye X, Zeng M, Zhao Q, Keefe DL, Liu L, Resveratrol protects against age-associated infertility in mice, Hum. Reprod 28 (3) (2013) 707–717. [PubMed: 23293221]

[35]. Chen Z-G, Luo L-L, Xu J-J, Zhuang X-L, Kong X-X, Fu Y-C, Effects of plant polyphenols on ovarian follicular reserve in aging rats, Biochem. Cell Biol 88 (4) (2010) 737–745. [PubMed: 20651847]

[36]. Banu SK, Stanley JA, Sivakumar KK, Arosh JA, Burghardt RC, Resveratrol protects the ovary against chromium-toxicity by enhancing endogenous antioxidant enzymes and inhibiting metabolic clearance of estradiol, Toxicol. Appl. Pharmacol 303 (2016) 65–78. [PubMed: 27129868]

[37]. Luo J, Nikolaev AY, i Imai S, Chen D, Su F, Shiloh A, Guarente L, Gu W, Negative control of p53 by Sir2α promotes cell survival under stress, Cell 107 (2) (2001) 137–148. [PubMed: 11672522]

[38]. Motta MC, Divecha N, Lemieux M, Kamel C, Chen D, Gu W, Bultsma Y, McBurney M, Guarente L, Mammalian SIRT1 represses forkhead transcription factors, Cell 116 (4) (2004) 551–563. [PubMed: 14980222]

[39]. Vaziri H, Dessain SK, Eaton EN, Imai S-I, Frye RA, Pandita TK, Guarente L, Weinberg RA, hSIR2SIRT1 functions as an NAD-dependent p53 deacetylase, Cell 107 (2) (2001) 149–159. [PubMed: 11672523]

[40]. Yeung F, Hoberg JE, Ramsey CS, Keller MD, Jones DR, Frye RA, Mayo MW, Modulation of NF-κB-dependent transcription and cell survival by the SIRT1 deacetylase, EMBO J. 23 (12) (2004) 2369–2380. [PubMed: 15152190]

[41]. Curtil C, Enache LS, Radreau P, Dron AG, Scholtes C, Deloire A, Roche D, Lotteau V, Andre P, Ramiere C, The metabolic sensors FXRalpha, PGC-1alpha, and SIRT1 cooperatively regulate hepatitis B virus transcription, FASEB J. 28 (3) (2014) 1454–1463. [PubMed: 24297698]

[42]. Canto C, Auwerx J, PGC-1alpha, SIRT1 and AMPK, an energy sensing network that controls energy expenditure, Curr. Opin. Lipidol 20 (2) (2009) 98–105. [PubMed: 19276888]

[43]. Austin S, St-Pierre J, PGC1alpha and mitochondrial metabolism–emerging concepts and relevance in ageing and neurodegenerative disorders, J. Cell Sci 125 (Pt 21) (2012) 4963–4971. [PubMed: 23277535]

[44]. Yuan W, Effects of resveratrol on oxidative stress in lead-induced AD-like lesions in mice, Zhengzhou Univ., 2014.

[45]. Chen D, Liu XH, Zeng XX, Gou QD, Xie C, Dong YT, et al. , Expression of silencing information regulators in brain tissue of rats with chronic fluorosis and its relationship with learning and memory ability, Zhong Guo Di Fang Bing Xue Za Zhi 37 (4) (2018) 265.

[46]. Tang BL, Sirt1 and the mitochondria, Mol. Cells 39 (2) (2016) 87. [PubMed: 26831453]

[47]. Kim D, Nguyen MD, Dobbin MM, Fischer A, Sananbenesi F, Rodgers JT, Delalle I, Baur JA, Sui G, Armour SM, Puigserver P, Sinclair DA, Tsai LH, SIRT1 deacetylase protects against neurodegeneration in models for Alzheimer's disease and amyotrophic lateral sclerosis, Embo J. 26 (13) (2007) 3169–3179. [PubMed: 17581637]

[48]. Qin W, Chachich M, Lane M, Roth G, Bryant M, de Cabo R, Ottinger MA, Mattison J, Ingram D, Gandy S, Pasinetti GM, Calorie restriction attenuates Alzheimer's disease type brain amyloidosis in Squirrel monkeys (Saimiri sciureus), J. Alzheimer's Dis. JAD 10 (4) (2006) 417–422. [PubMed: 17183154]

[49]. Huang K, Huang J, Xie X, Wang S, Chen C, Shen X, Liu P, Huang H, Sirt1 resists advanced glycation end products-induced expressions of fibronectin and TGF-beta1 by activating the Nrf2/ARE pathway in glomerular mesangial cells, Free Rad. Biol. Med 65 (2013) 528–540. [PubMed: 23891678]

[50]. Pearson M, Carbone R, Sebastiani C, Cioce M, Fagioli M, Saito S, Higashimoto Y, Appella E, Minucci S, Pandolfi PP, Pelicci PG, PML regulates p53 acetylation and premature senescence induced by oncogenic Ras, Nature 406 (6792) (2000) 207–210. [PubMed: 10910364]

[51]. Langley E, Pearson M, Faretta M, Bauer UM, Frye RA, Minucci S, Pelicci PG, Kouzarides T, Human SIR2 deacetylates p53 and antagonizes PML/p53-induced cellular senescence, EMBO J. 21 (10) (2002) 2383–2396. [PubMed: 12006491]

[52]. Vengosh A, Coyte R, Karr J, Harkness JS, Kondash AJ, Ruhl LS, Merola RB, Dywer GS, Origin of hexavalent chromium in drinking water wells from the piedmont aquifers of North Carolina, Environ. Sci. Technol. Lett 3 (12) (2016) 409–414.

[53]. Singh R, Sengupta B, Bali R, Shukla B, Gurunadharao V, Srivatstava R, Identification and mapping of chromium (VI) plume in groundwater for remediation: a case study at Kanpur, Uttar Pradesh, J. Geol. Soc. India 74 (1) (2009) 49–57.

[54]. Sutherland JE, Zhitkovich A, Kluz T, Costa M, Rats retain chromium in tissues following chronic ingestion of drinking water containing hexavalent chromium, Biol. Trace Elem. Res 74 (1) (2000) 41–53. [PubMed: 11049199]

[55]. Stein LS, Stoica G, Tilley R, Burghardt RC, Rat ovarian granulosa cell culture: a model system for the study of cell-cell communication during multistep transformation, Cancer Res. 51 (2) (1991) 696–706. [PubMed: 1845958]

[56]. Wang C-J, Zhou Z-G, Holmqvist A, Zhang H, Li Y, Adell G, Sun X-F, Survivin expression quantified by Image Pro-Plus compared with visual assessment, Appl. Immunohistochem. Mol. Morphol 17 (6) (2009) 530–535. [PubMed: 19407655]

[57]. Banu SK, Stanley JA, Sivakumar KK, Arosh JA, Barhoumi R, Burghardt RC, Identifying a novel role for X-prolyl aminopeptidase (Xpnpep) 2 in CrVI-induced adverse effects on germ cell nest breakdown and follicle development in rats, Biol. Reprod 92 (3) (2015) 1–18.

[58]. Sivakumar KK, Stanley JA, Arosh JA, Pepling ME, Burghardt RC, Banu SK, Prenatal exposure to chromium induces early reproductive senescence by increasing germ cell apoptosis and advancing germ cell cyst breakdown in the F1 offspring, Dev. Biol 388 (1) (2014) 22–34. [PubMed: 24530425]

[59]. Hewitt SM, Baskin DG, Frevert CW, Stahl WL, Rosa-Molinar E, Controls for immunohistochemistry: the Histochemical Society's standards of practice for validation of immunohistochemical assays, J. Histochem. Cytochem 62 (10) (2014) 693–697. [PubMed: 25023613]

[60]. Lee J, Banu SK, Burghardt RC, Starzinski-Powitz A, Arosh JA, Selective inhibition of prostaglandin E2 receptors EP2 and EP4 inhibits adhesion of human endometriotic epithelial and stromal cells through suppression of integrin-mediated mechanisms, Biol. Reprod 88 (3) (2013), 77–77. [PubMed: 23242524]

[61]. Kratzer DD, Littell RC, Appropriate statistical methods to compare dose responses of methionine sources, Poult. Sci 85 (5) (2006) 947–954. [PubMed: 16673777]

[62]. Solomon JM, Pasupuleti R, Xu L, McDonagh T, Curtis R, DiStefano PS, Huber LJ, Inhibition of SIRT1 catalytic activity increases p53 acetylation but does not alter cell survival following DNA damage, Mol. Cell. Biol 26 (1) (2006) 28–38. [PubMed: 16354677]

[63]. Stanley JA, Arosh JA, Burghardt RC, Banu SK, A fetal whole ovarian culture model for the evaluation of CrVI-induced developmental toxicity during germ cell nest breakdown, Toxicol. Appl. Pharmacol 289 (1) (2015) 58–69. [PubMed: 26348139]

[64]. Banu SK, Stanley JA, Sivakumar KK, Arosh JA, Taylor RJ, Burghardt RC, Chromium VI - induced developmental toxicity of placenta is mediated through spatiotemporal dysregulation of cell survival and apoptotic proteins, Reprod. Toxicol 68 (2017) 171–190. [PubMed: 27443218]

[65]. Nguyen Q-N, Zerafa N, Liew SH, Morgan FH, Strasser A, Scott CL, Findlay JK, Hickey M, Hutt KJ, Loss of PUMA protects the ovarian reserve during DNA-damaging chemotherapy and preserves fertility, Cell Death Dis. 9 (6) (2018) 1–12. [PubMed: 29298988]

[66]. Li M, The role of P53 up-regulated modulator of apoptosis (PUMA) in ovarian development, cardiovascular and neurodegenerative diseases, Apoptosis 26 (5) (2021) 235–247. [PubMed: 33783663]

[67]. Edlich F, BCL-2 proteins and apoptosis: recent insights and unknowns, Biochem. Biophys. Res. Commun 500 (1) (2018) 26–34. [PubMed: 28676391]

[68]. Flaws JA, Hirshfield AN, Hewitt JA, Babus JK, Furth PA, Effect of bcl-2 on the primordial follicle endowment in the mouse ovary, Biol. Reprod 64 (4) (2001) 1153–1159. [PubMed: 11259262]

[69]. Jääskeläinen M, Nieminen A, Pökkylä R-M, Kauppinen M, Liakka A, Heikinheimo M, Vaskivuo TE, Klefström J, Tapanainen JS, Regulation of cell death in human fetal and adult ovaries—role of Bok and Bcl-XL, Mol. Cell. Endocrinol 330 (1–2) (2010) 17–24. [PubMed: 20673843]

[70]. Ratts VS, Flaws JA, Kolp R, Sorenson CM, Tilly J, Ablation of bcl-2 gene expression decreases the numbers of oocytes and primordial follicles established in the post-natal female mouse gonad, Endocrinology 136 (8) (1995) 3665–3668. [PubMed: 7628407]

[71]. Makker A, Goel MM, Mahdi AA, PI3K/PTEN/Akt and TSC/mTOR signaling pathways, ovarian dysfunction, and infertility: an update, J. Mol. Endocrinol 53 (3) (2014) 103–118.

[72]. Song G, Ouyang G, Bao S, The activation of Akt/PKB signaling pathway and cell survival, J. Cell. Mol. Med 9 (1) (2005) 59–71. [PubMed: 15784165]

[73]. Li M, Luo J, Brooks CL, Gu W, Acetylation of p53 inhibits its ubiquitination by Mdm2, J. Biol. Chem 277 (52) (2002) 50607–50611. [PubMed: 12421820]

[74]. Albamonte MS, Willis MA, Albamonte MI, Jensen F, Espinosa MB, Vitullo AD, The developing human ovary: immunohistochemical analysis of germ-cell-specific VASA protein, BCL-2/BAX expression balance and apoptosis, Hum. Reprod 23 (8) (2008) 1895–1901. [PubMed: 18534994]

[75]. Reddy P, Shen L, Ren C, Boman K, Lundin E, Ottander U, Lindgren P, x Liu Y, y Sun Q, Liu K, Activation of Akt (PKB) and suppression of FKHRL1 in mouse and rat oocytes by stem cell factor during follicular activation and development, Dev. Biol 281 (2) (2005) 160–170. [PubMed: 15893970]

[76]. Lee BB, Kim Y, Kim D, Cho EY, Han J, Kim HK, Shim YM, Kim DH, Metformin and tenovin-6 synergistically induces apoptosis through LKB1–independent SIRT1 down-regulation in non-small cell lung cancer cells, J. Cell. Mol. Med 23 (4) (2019) 2872–2889. [PubMed: 30710424]

[77]. Zhang Y, et al. , PUMA promotes Bax translocation by both directly interacting with Bax and by competitive binding to Bcl-XL during UV-induced apoptosis, Molecular biology of the cell 20 (13) (2009) 3077–3087, 10.1091/mbc.e08-11-1109. [PubMed: 19439449]

[78]. Rucker III EB, Dierisseau P, Wagner K-U, Garrett L, Wynshaw-Boris A, Flaws JA, Hennighausen L, Bcl-x and Bax regulate mouse primordial germ cell survival and apoptosis during embryogenesis, Molecular endocrinology 14 (7) (2000) 1038–1052. [PubMed: 10894153]

[79]. Greenfeld CR, Babus JK, Furth PA, Marion S, Hoyer PB, A Flaws J, BAX is involved in regulating follicular growth, but is dispensable for follicle atresia in adult mouse ovaries, Reproduction 133 (1) (2007) 107–116. [PubMed: 17244737]

Highlights

- Prenatal Cr(VI) exposure accelerated oocytes apoptosis in F1 offspring.
- Inhibition of sirtuin1 exacerbated Cr(VI) toxicity in the F1 ovary synergistically.
- Cr(VI) altered the p53:SIRT1 ratio in the ovary and inhibited p53-SIRT1 interaction in the ovarian granulosa cell line.
- Cr(VI) and sirtuin1 inhibitor hyperacetylated p53 ensuring p53-stabilization in the ovary of the F1 offspring.
- Cr(VI)-p53 partner together in oocyte apoptosis to activate PUMA, Bax, and caspase-3 and inhibit AKT, Bcl-2, and Bcl-XL.

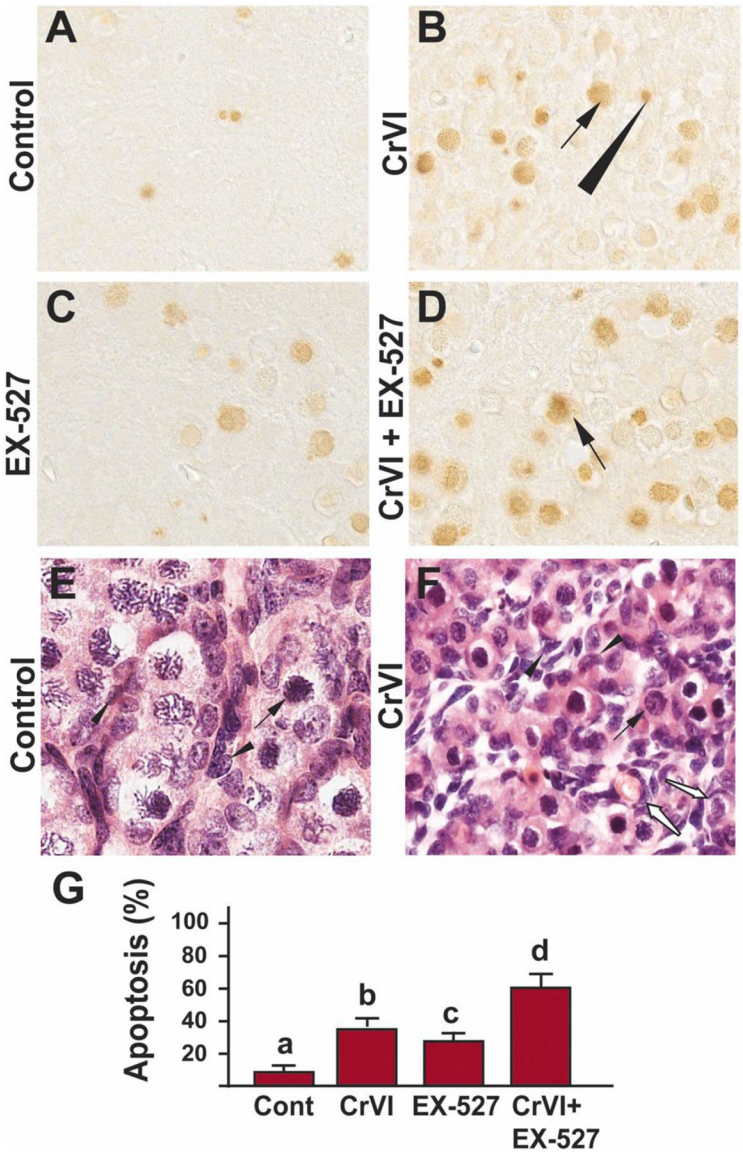

Fig. 1.

SIRT1 inhibitor exacerbated Cr(VI)-induced germ cell apoptosis of F1 offspring. Pregnant dams (F0) were exposed to Cr(VI) (10 ppm) through drinking water from 9.5–14.5 days *post-coitum* (dpc). Cr(VI) exposed and unexposed dams were injected (*i.p.)* with EX-527 (50 mg/kg body weight). On postnatal day (PND) 1, F1 offspring were euthanized, and ovaries were processed for TUNEL assay as described under *Materials and methods*. Representative images of the ovaries are shown from control (A), Cr(VI) (B), EX-527 (C), and Cr(VI)+EX-527 (D). H&E images of control (E) and Cr(VI)-exposed (F) ovaries are shown. The histogram shows the percentage of TUNEL-positive apoptotic cells (G). Different lowercase letters (a, b, c, d) indicate significant differences between groups ($p<0.05$). Each value is mean ± SEM 5 F0 rats (n=5). Arrows (germ cells) and arrowhead (somatic cell) indicate apoptotic TUNEL-positive cells, white arrows (F) show partly formed primordial follicles.

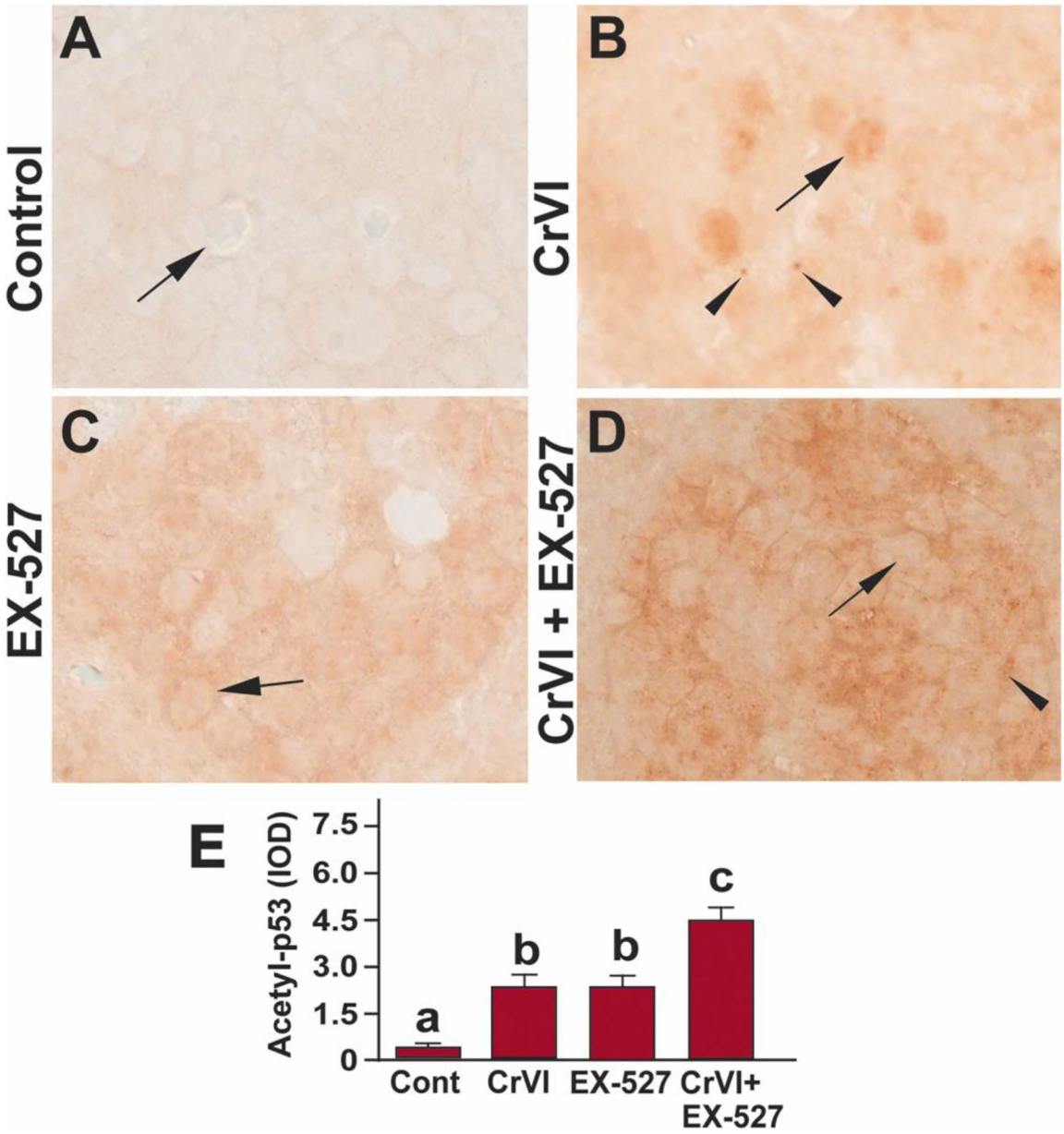

Fig. 2.

SIRT1 inhibitor hyperacetylated p53(K-382) in the ovary of F1 offspring. Pregnant dams (F0) were exposed to Cr(VI) (10 ppm) through drinking water from 9.5–14.5 days *post-coitum* (dpc). Cr(VI) exposed and unexposed dams were injected (*i.p.)* with EX-527 (50 mg/kg body weight). On postnatal day (PND) 1, F1 offspring were euthanized, and ovaries were processed for Immunohistochemistry (IHC). Representative images of the ovaries are shown from control (A), Cr(VI) (B), EX-527 (C), and Cr(VI)+EX-527 (D). The histogram shows the integrated optical density (IOD) (E). Different lowercase letters (a, b, c, d) indicate significant differences between groups ($p<0.05$). There are no significant differences between groups marked by the same letter. Each value is mean ± SEM 5 F0 rats (n=5). Arrows indicate germ cells, and the arrowhead indicates a somatic cell.

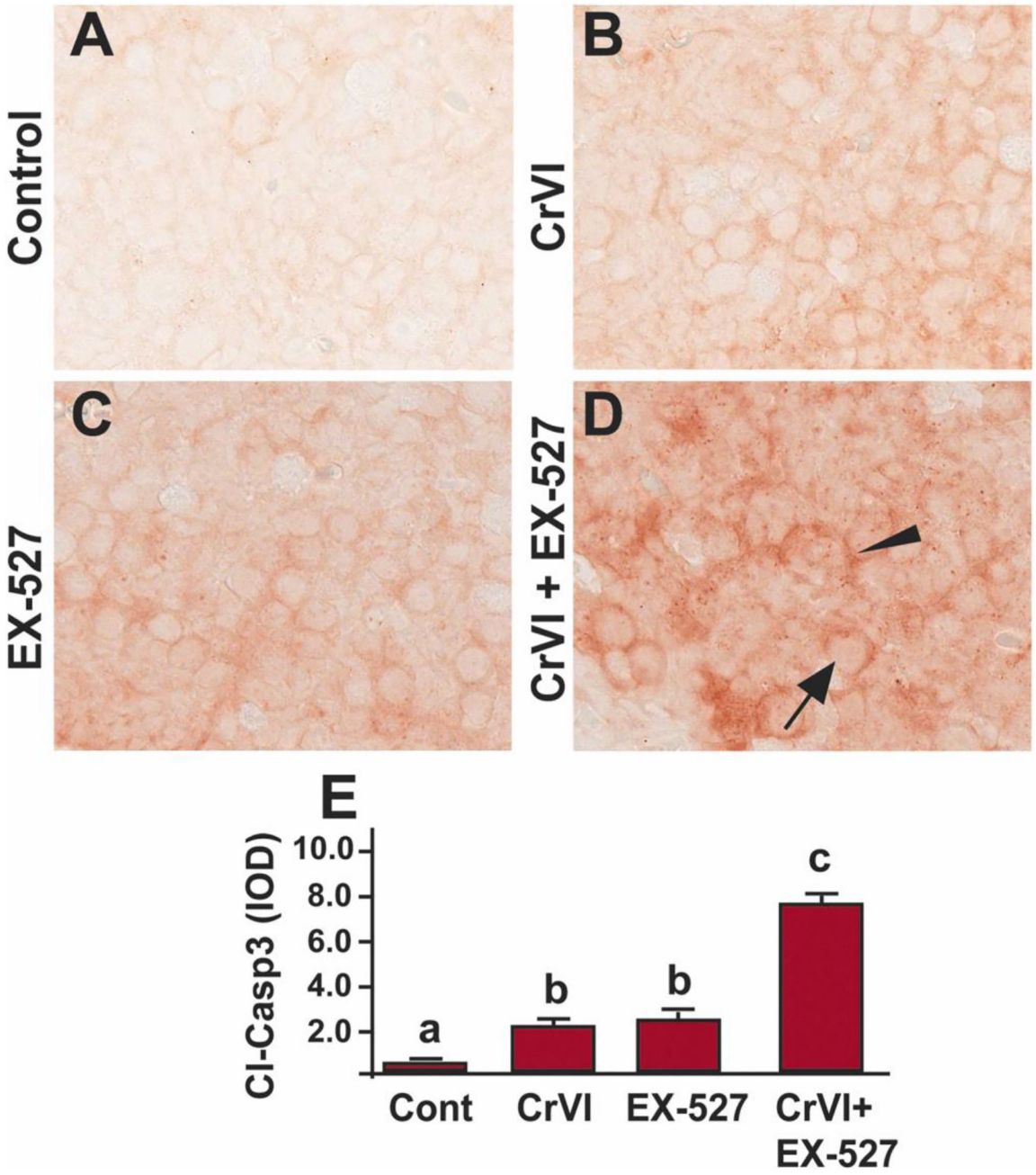

Fig. 3.

SIRT1 inhibitor increased cleaved-caspase-3 in the ovary of F1 offspring. Pregnant dams (F0) were exposed to Cr(VI) (10 ppm) through drinking water from 9.5–14.5 dpc. Cr(VI) exposed and unexposed dams were injected (*i.p.)* with EX-527 (50 mg/kg body weight). On PND1, the F1 offspring were euthanized, and ovaries were processed for IHC. Representative images of the ovaries are shown from control (A), Cr(VI) (B), EX-527 (C), and Cr(VI)+EX-527 (D). The histogram shows the integrated optical density (IOD) (E). Different lowercase letters (a, b, c) indicate significant differences between groups ($p<0.05$). There are no significant differences between groups marked by the same letter. Each value

is mean ± SEM 5 F0 rats (n=5). Arrow indicates germ cell, and the arrowhead indicates a somatic cell.

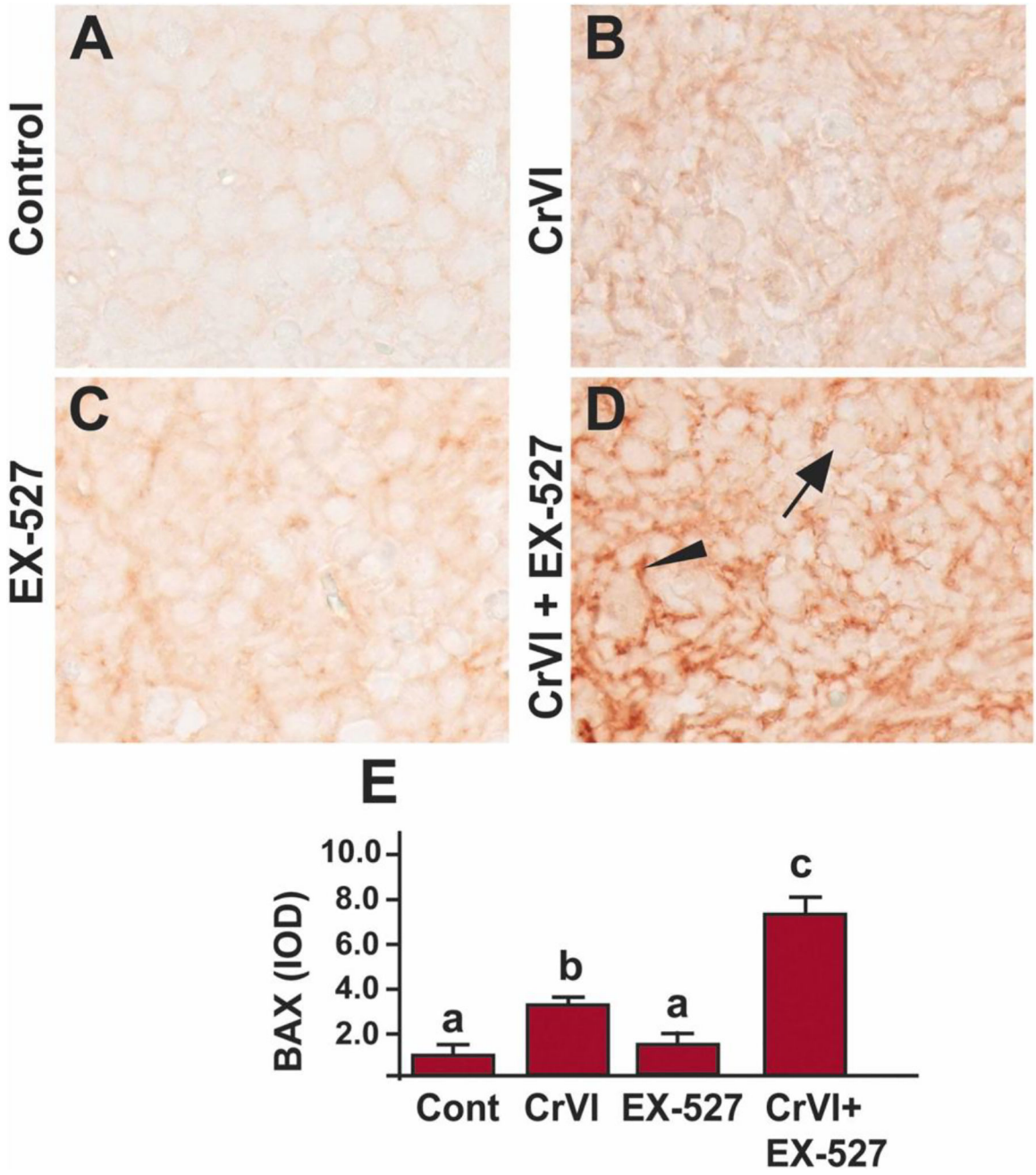

Fig. 4.

SIRT1 inhibitor increased BAX in the ovary of F1 offspring. Pregnant dams (F0) were exposed to Cr(VI) (10 ppm) through drinking water from 9.5–14.5 days *post-coitum* (dpc). Cr(VI) exposed and unexposed dams were injected (*i.p.)* with EX-527 (50 mg/kg body weight). On postnatal day (PND) 1, F1 offspring were euthanized, and ovaries were processed for IHC. Representative images of the ovaries are shown from control (A), Cr(VI) (B), EX-527 (C), and Cr(VI)+EX-527 (D). The histogram shows the integrated optical density (IOD) (E). Different lowercase letters (a, b, c) indicate significant differences between groups ($p<0.05$). There are no significant differences between groups marked by

the same letter. Each value is mean ± SEM 5 F0 rats (n=5). Arrow indicates germ cell, and the arrowhead indicates a somatic cell.

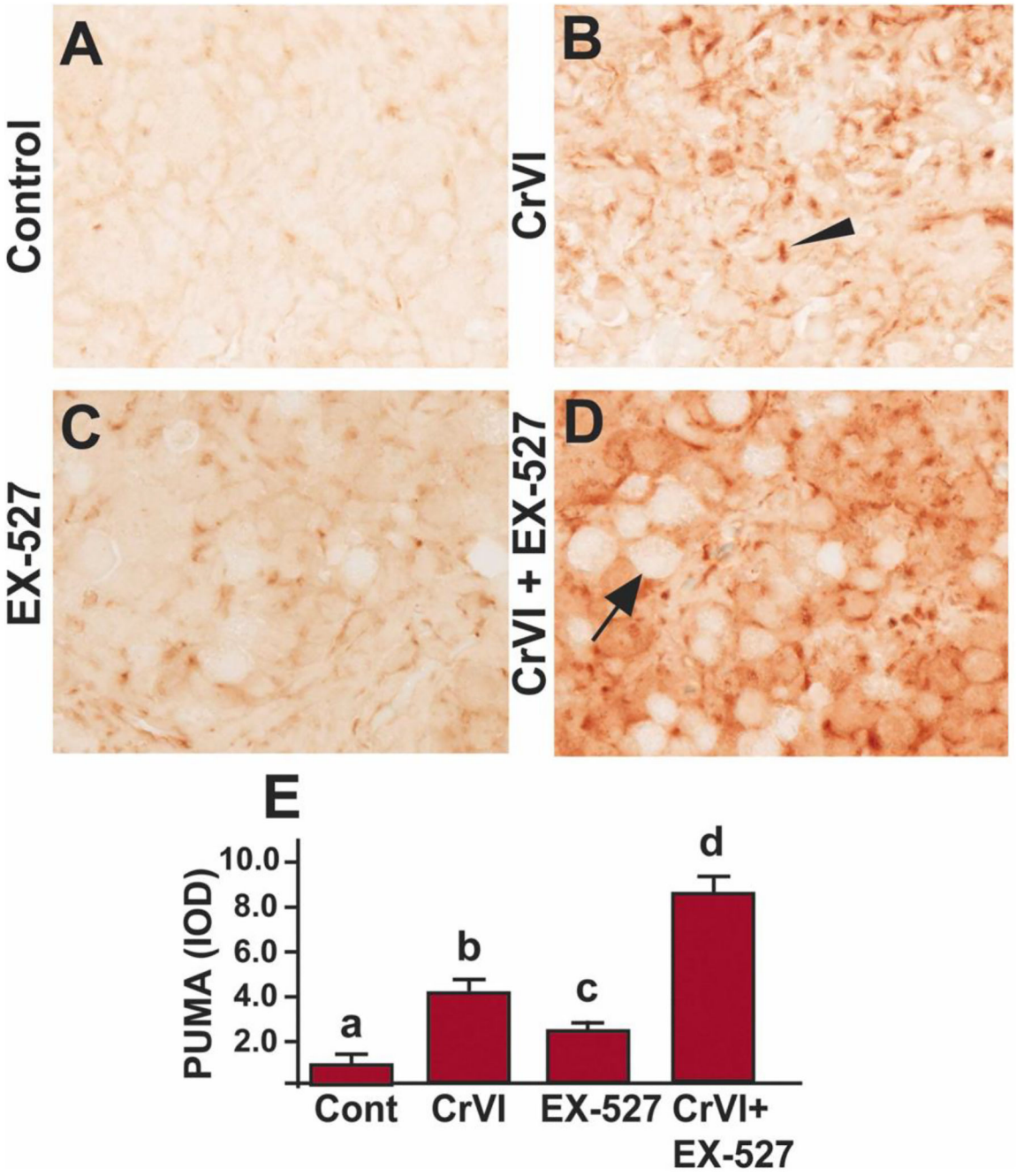

Fig. 5.

SIRT1 inhibitor increased PUMA in the ovary of F1 offspring. Pregnant dams (F0) were exposed to Cr(VI) (10 ppm) through drinking water from 9.5–14.5 days *post-coitum* (dpc). Cr(VI) exposed and unexposed dams were injected (*i.p.)* with EX-527 (50 mg/kg body weight). On postnatal day (PND) 1, F1 offspring were euthanized, and ovaries were processed for IHC. Representative images of the ovaries are shown from control (A), Cr(VI) (B), EX-527 (C), and Cr(VI)+EX-527 (D). The histogram shows the integrated optical density (IOD) (E). Different lowercase letters (a, b, c, d) indicate significant differences

between groups ($p<0.05$). Each value is mean ± SEM 5 F0 rats (n=5). Arrow indicates germ cell, and the arrowhead indicates a somatic cell.

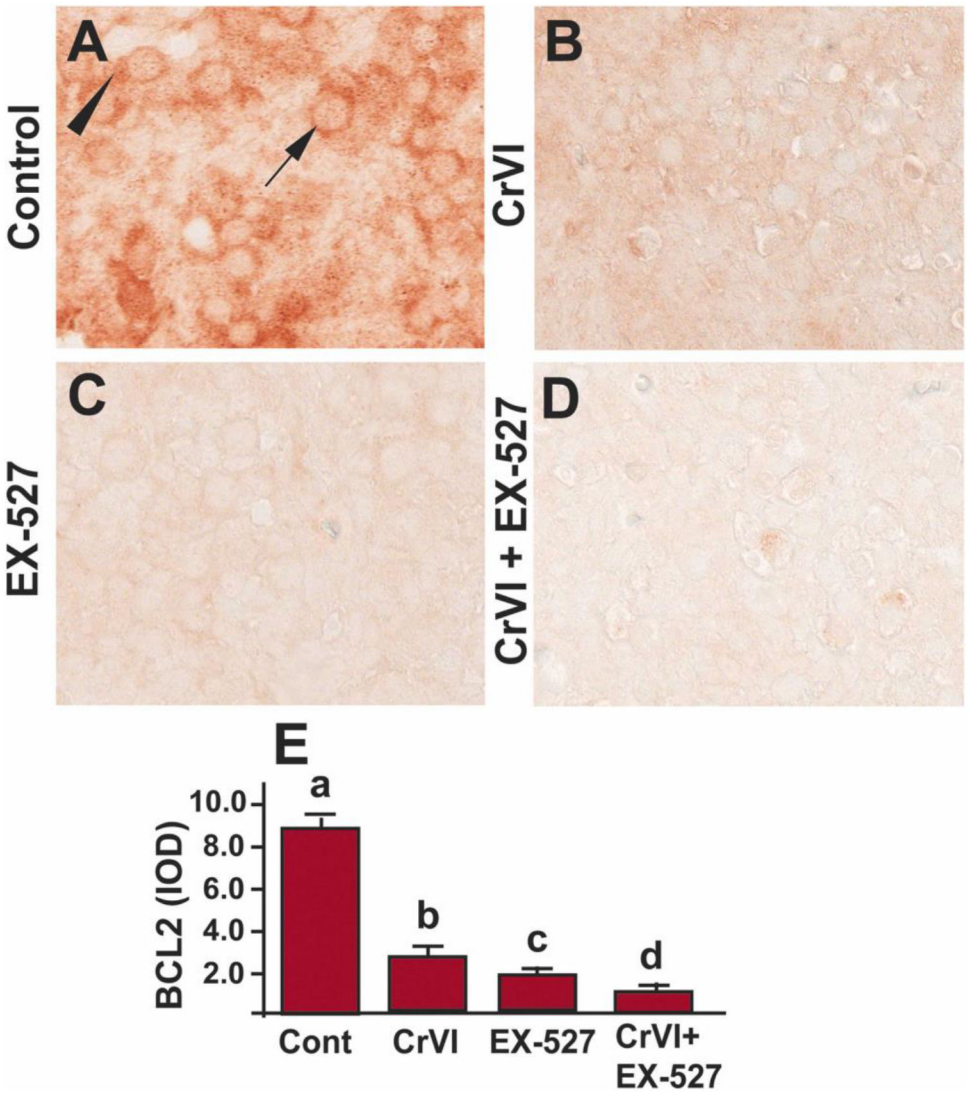

Fig. 6.

SIRT1 inhibitor decreased Bcl-2 in the ovary of F1 offspring. Pregnant dams (F0) were exposed to Cr(VI) (10 ppm) through drinking water from 9.5–14.5 dpc. Cr(VI) exposed and unexposed dams were injected (*i.p.)* with EX-527 (50 mg/kg body weight). On PND1, the F1 offspring were euthanized, and ovaries were processed for IHC. Representative images of the ovaries are shown from control (A), Cr(VI) (B), EX-527 (C), and Cr(VI)+EX-527 (D). The histogram shows the integrated optical density (IOD) (E). Different lowercase letters (a, b, c, d) indicate significant differences between groups ($p<0.05$). Each value is mean ± SEM 5 F0 rats (n=5). Arrow indicates germ cell, and the arrowhead indicates a somatic cell.

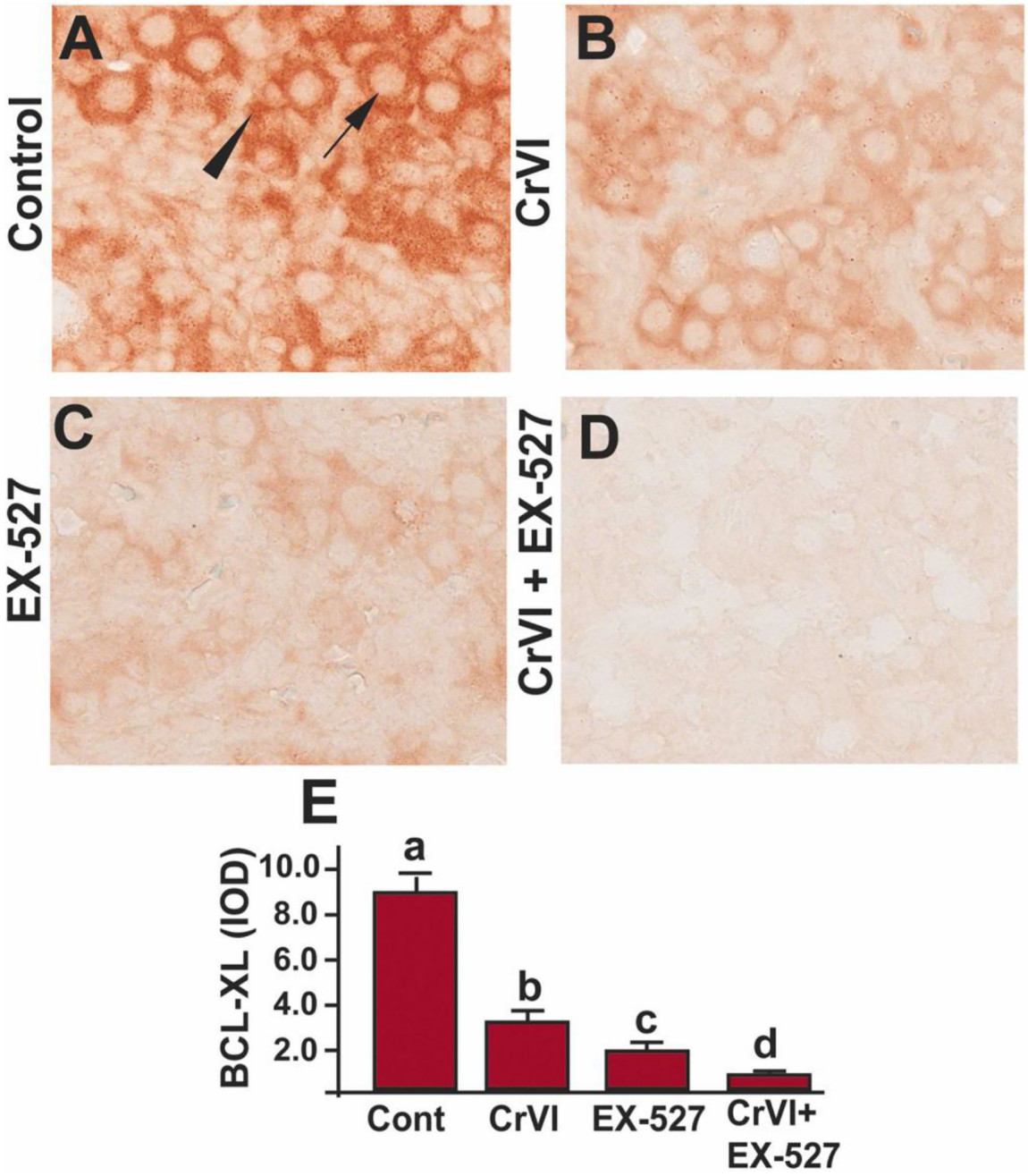

Fig. 7.

SIRT1 inhibitor decreased Bcl-XL in the ovary of F1 offspring. Pregnant dams (F0) were exposed to Cr(VI) (10 ppm) through drinking water from 9.5–14.5 days *post-coitum* (dpc). Cr(VI) exposed and unexposed dams were injected (*i.p.)* with EX-527 (50 mg/kg body weight). On postnatal day (PND) 1, F1 offspring were euthanized, and ovaries were processed for IHC. Representative images of the ovaries are shown from control (A), Cr(VI) (B), EX-527 (C), and Cr(VI)+EX-527 (D). The histogram shows the integrated optical density (IOD) (E). Different lowercase letters (a, b, c, d) indicate significant differences

between groups ($p<0.05$). Each value is mean ± SEM 5 F0 rats (n=5). Arrow indicates germ cell, and the arrowhead indicates a somatic cell.

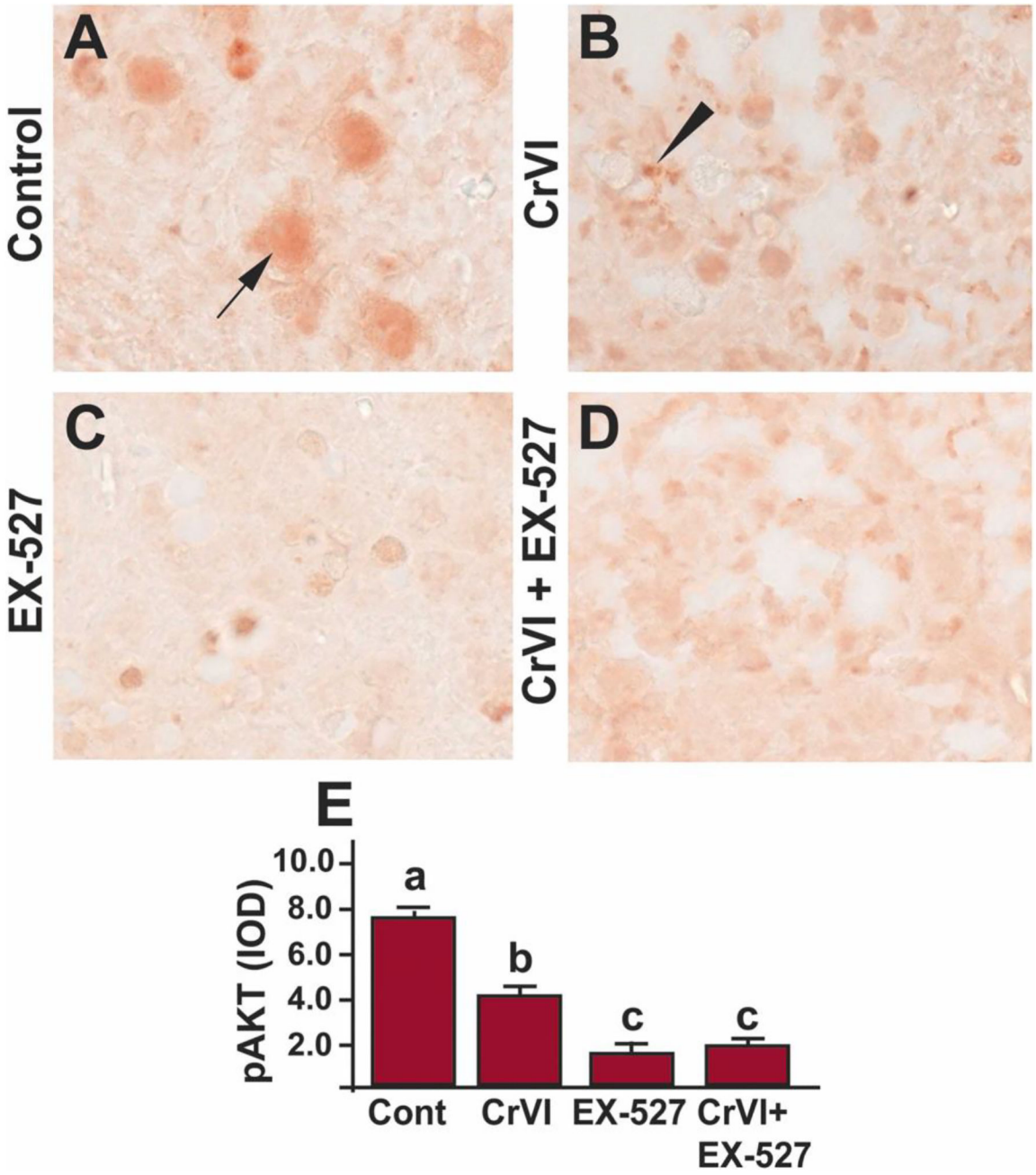

Fig. 8.

SIRT1 inhibitor decreased p-AKT in the ovary of F1 offspring. Pregnant dams (F0) were exposed to Cr(VI) (10 ppm) through drinking water from 9.5–14.5 dpc. Cr(VI) exposed and unexposed dams were injected (*i.p.)* with EX-527 (50 mg/kg body weight). On PND1, the F1 offspring were euthanized, and ovaries were processed for IHC. Representative images of the ovaries are shown from control (A), Cr(VI) (B), EX-527 (C), and Cr(VI)+EX-527 (D). The histogram shows the integrated optical density (IOD) (E). Different lowercase letters (a, b, c) indicate significant differences between groups ($p<0.05$). There are no significant

differences between groups marked by the same letter. Each value is mean ± SEM 5 F0 rats (n=5). Arrow indicates germ cell, and the arrowhead indicates a somatic cell.

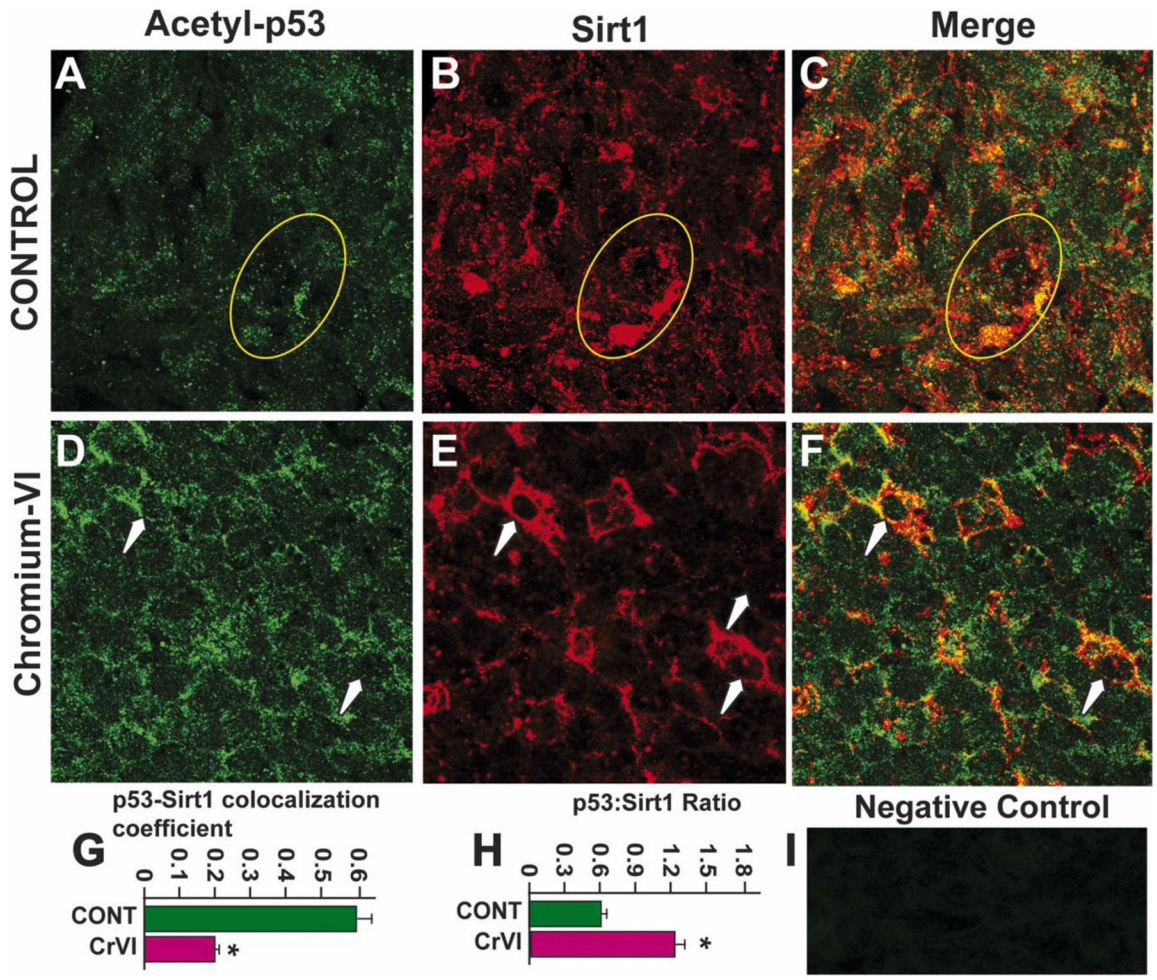

Fig. 9.

Cr(VI) increased acetyl-p53:SIRT1 co-localization and ratio in the ovary of F1 offspring. Cr(VI) increased the co-localization of acetyl-p53 and SIRT1 in the germ cells and somatic cells of the PND1 ovary. Pregnant dams were treated with or without Cr(VI) (10 ppm) through drinking water from 9.5–14.5 days post-coitum (dpc). On postnatal day (PND) 1, F1 offspring were euthanized, and ovaries were processed for immunofluorescence. Representative images of the ovaries are shown from control (A - p53; B - SIRT1; C - Merge) and Cr(VI) (D - acetyl p53; E - SIRT1; F - Merge). Histograms show acetyl-p53:SIRT1 co-localization (G) and p53:SIRT1 ratio (H). I - Negative control. * Control *vs.* Cr(VI) ($p<0.05$).

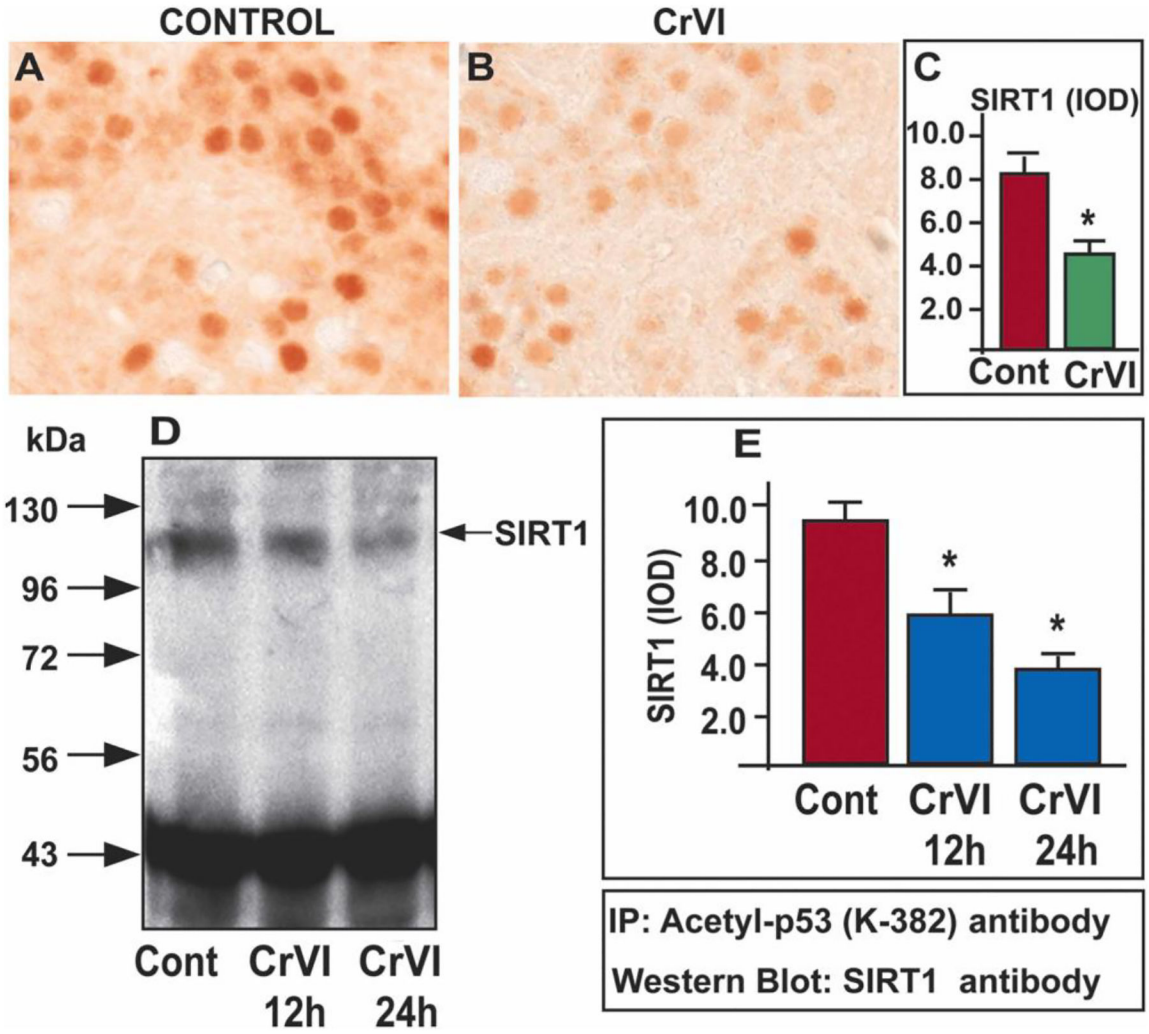

Fig. 10.

Cr(VI) decreased acetyl-p53-SIRT1 interaction. Pregnant dams were exposed to Cr(VI) (10 ppm) through drinking water from 9.5–14.5 *dpc*. On PND1, the F1 offspring were euthanized, and ovaries were processed for IHC. Representative images of the ovaries are shown from control (A) and Cr(VI) treatment (B). The histogram shows the integrated optical density (IOD) (C). * Control *vs*. Cr(VI), $p<0.05$. Spontaneously Immortalized rat Granulosa Cells (SIGC) were cultured as described under materials and methods and treated with Cr(VI) (25 μM potassium dichromate) for 12 or 24 h. IP was performed with acetyl-p53 antibody and western blot with SIRT1 antibody (D). The histogram shows IOD of SIRT1 expression by the western blot: 0 h (treated with media alone), 12 and 24 h (treated with Cr(VI) for 12 or 24 h) (E). * Control *vs*. Cr(VI) treatment for 12 or 24 h ($p<0.05$).

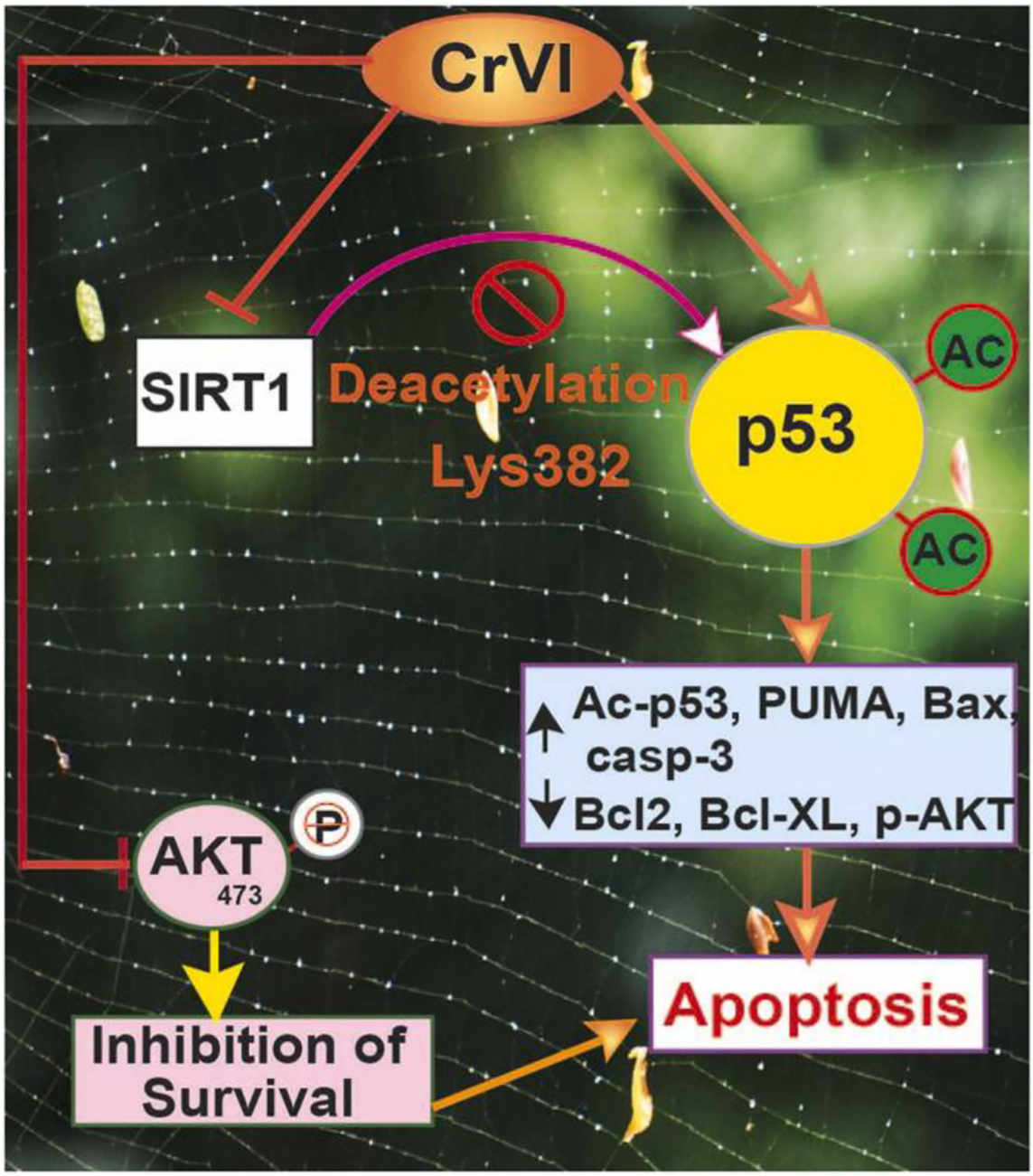

Fig. 11.
Schematic diagram of the mechanism of SIRT1-acetyl p53 network in mediating apoptosis in the ovary.

Table 1.

Antibody Table (Source, catalog numbers, dilutions, host species and Immunogen)

S.No	Peptide/ protein target	Immunogen	Name of Antibody	Manufacturer; catalog #	Species raised in	Dilution used
1	Acetyl-p53	Synthetic peptide conjugated to KLH derived from within residues 350 to the C-terminus of Human p53	Rabbit-Anti-p53 (acetyl K382)	Abcam; Ab37318	Rabbit polyclonal	1:100
2	PUMA	Synthetic peptide corresponding to C terminal amino acids 180–193 (PLPRGHR APEMEPN) of Human PUMA alpha	Rabbit Anti-PUMA	Abcam; Ab9643	Rabbit polyclonal	1:1000
3	BAX	Synthesized peptide derived from human BAX	Rabbit Anti-BAX	Sigma; SAB4502549	Rabbit polyclonal	1:1500
4	Cleaved-Caspase-3	Synthetic peptide corresponding to amino-terminal residues adjacent to (Asp175) in human caspase-3	Rabbit Anti-Cleaved-Caspase-3	Cell Signaling; 9661	Rabbit polyclonal	1:300
5	BCL2	N terminal amino acids 1–18 of Human BCL-2; AGRTGYDNREIVMKYIHY	Rabbit Anti-BCL-2	Abcam; ab7973	Rabbit polyclonal	1:250
6	BCL-XL	Synthetic peptide corresponding to residues surrounding Asp61 of human BCL-XL	Rabbit Anti-BCL-XL	Cell Signaling; 2762	Rabbit polyclonal	1:200
7	p-AKT	Synthetic phosphopeptide corresponding to residues surrounding Ser473 of mouse AKT.	Rabbit Anti-phospho AKT (Ser473)	Cell Signaling; 3787	Rabbit monoclonal	1:50
8	SIRT-1	Recombinant Human SIRT1	Mouse Anti-SIRT1	Abcam; Ab110304	Mouse monoclonal	1:100